Below-barrier fusion of complex nuclei

V. P. Permyakov and V. M. Shilov

Joint Institute for Nuclear Research, Dubna

Fiz. Elem. Chastits At. Yadra **20**, 1396–1438 (November–December 1989)

Theoretical models for describing the cross sections for total fusion of light and intermediate nuclei at below-barrier and near-barrier energies are considered. A multichannel model with boundary conditions in the form of a converging wave in the interior region of the nucleus is discussed in detail, and various simplifications of the model are considered. Further, the elastic and inelastic cross sections are treated on a common basis, and the decay properties of compound nuclei are discussed. A comparison with experimental data is made.

INTRODUCTION

Although quantum-mechanical tunneling is a well-known and widely used phenomenon not only in nuclear physics but also in other sciences,[1] investigations of tunneling in complex nuclear systems are still among the most topical problems for theory and experiment.[2]

An important problem, for example, is still the extrapolation of near-barrier data on the cross sections for fusion of carbon and oxygen nuclei to the region of astrophysical energies. These processes govern the evolution of stars at the late stages of their evolution.[3]

Tunneling below the Coulomb barrier also determines the lifetimes of heavy nuclei against α decay[4] and against decay with emission of heavy clusters.[5]

Below-barrier fusion is an attractive process for obtaining superheavy compound nuclei with minimal excitation energy, reducing the probability of decay of these nuclei through the fission channel.[6]

When two ions fuse, they form a system with a certain excitation energy and angular momentum. This system will then be de-excited by the emission of light particles and photons, becoming a cold residual nucleus. For heavy compound nuclei, for which the fission barrier is low or greatly reduced by the introduction of a large amount of angular momentum, the fission channel is also open. Thus, the experimental fusion cross section σ_{fus} can be obtained from a sum of two terms: the evaporation cross section and the fission cross section.

In accordance with Bohr's definition of a compound nucleus, the compound system must achieve complete equilibrium with respect to all degrees of freedom. The only quantities that characterize such a system are its charge, mass, energy, and angular momentum. Compound nuclei must decay in accordance with the laws of statistical mechanics,[7] and these laws impose certain requirements on the energy, angular, and mass distributions of the evaporating particles and fission fragments.

In this review we have restricted our analysis to systems formed by the fusion of not too heavy nuclei having product of the charges $Z_1 Z_2 < 2000$. For nuclei that do not satisfy this condition, the fusion threshold energy is predicted[8] to be much higher than for the total reaction cross section σ_r, and in this case new reaction channels, called direct fission,[9] "quasifission,"[10] and fast fission,[11] are open. Experimentally, it is difficult to distinguish such processes from the decay of a true compound nucleus, and their discussion requires a separate paper.

We shall also omit discussion of how the total-fusion channel is distinguished experimentally from the many competing reaction channels, and by "fusion" we shall mean throughout the paper a process of formation of a compound nucleus with the establishment of statistical equilibrium with respect to all the degrees of freedom.

The fusion of two heavy ions at near-barrier energies can be described well in the framework of a simple one-dimensional model. The fusion cross section is determined by the probability for tunneling through a potential that is the sum of the nuclear, Coulomb, and centrifugal potentials of the two colliding ions. An enormous number of studies have been made in the framework of this model (see, for example, the review of Ref. 12). Because the one-dimensional model is the basis for the subsequent development of the theory, we consider in the next section the foundations of this model, together with typical experimental data.

As the sensitivity of the experimental fissilities was improved, it became possible to investigate fusion cross sections at below-barrier energies. The first such experiments,[13,14] made in 1980, led to unexpected results. The below-barrier fusion cross sections were found to be an order of magnitude and more greater than the theoretical estimates obtained in the framework of one-dimensional models.

It was later shown, in many studies,[15–21] that this enhancement of below-barrier fusion can be entirely adequately described if the internal structure of the colliding nuclei is taken into account properly. The multidimensional models developed in this connection also predicted that the compound nuclei that are formed should populate a much broader range of L values than what follows from the one-dimensional models, and this is confirmed experimentally. In Sec. 2 we consider the theoretical models that are currently used to describe processes of below-barrier tunneling.

The method of strong channel coupling used in multidimensional models encounters great computational difficulties in the case of intermediate and heavy nuclei, in which many channels are open. We shall therefore devote much attention to approximations that simplify the solution of the multichannel problem and permit qualitative estimates to be made.

In Sec. 3, we shall formulate, in the framework of multichannel models, boundary conditions for the description of processes that are the inverse of fusion, i.e., spontaneous decay and decay from excited states of heavy nuclei with emission of massive clusters. We shall demonstrate the asymmetry of the Coulomb-barrier penetrability in decay and in

 0090-4759/89/060594-19$04.40

fusion when allowance is made for the complex structure of the colliding nuclei. A simple method for qualitative explanation of this effect is proposed.

1. ONE-DIMENSIONAL MODELS

In the one-dimensional models there is an "effective" potential, a sum of the nuclear, Coulomb, and centrifugal potentials of the two colliding ions:

$$V_L(r) = V_{\text{Coul}}(r) + V_{\text{nuc}}(r) + L(L+1)\hbar^2/(2\mu r^2), \quad (1)$$

where L is the orbital angular momentum, and μ is the reduced mass of the system. (To simplify the exposition, we shall use the expressions for spinless nuclei throughout the review.) In such a model, the fusion cross section for the partial wave with angular momentum L is determined by the probability for the particle to pass through the Coulomb barrier determined by the expression (1). In terms of the partial waves, the fusion cross section can be expressed as

$$\sigma_{\text{fus}}(E) = \frac{\pi}{k^2}\sum_L (2L+1)\, T_L(E)\, P_L(E). \quad (2)$$

Here, k is the asymptotic wave number, $k = (2\mu E/\hbar^2]^{1/2}$; $T_L(E)$ is the penetrability of the "effective" potential (1) at energy E of the incident ions in the center-of-mass system, and $P_L(E)$ is the probability for the system to go over to the complete-fusion channel after passing the Coulomb barrier.

When fusion reactions are described in the one-dimensional models in the near-barrier region of energies for not too heavy nuclei, it is assumed that particles which overcome the Coulomb barrier necessarily fuse,[12] i.e., the probabilities are $P_L(E) = 1$, and that no kinetic energy is dissipated before the Coulomb barrier is passed.

In classical physics, the partial penetrabilities are completely determined by the height V_{b_L} of the barrier in the potential (1):

$$T_L(E) = \begin{cases} 1 & E > V_{b_L} \\ 0 & E < V_{b_L} \end{cases}. \quad (3)$$

In this case, the series (2) can be readily summed, and we obtain

$$\sigma_{\text{fus}} = \frac{\pi}{k^2}(L_{\text{cr}}+1)^2, \quad (4)$$

where L_{cr} is the last partial wave for which $E > V_{b_L}$. [The expression (4) is often used in the literature to represent the fusion cross sections in terms of the critical angular momentum L_{cr}, and the expression (3) for the penetrability is called the sharp-cutoff model.]

If, further, it is assumed that the barrier radius R_{b_L} does not depend on L and $L_{\text{cr}}(L_{\text{cr}}+1) \approx (L_{\text{cr}}+1)^2$, then we obtain the well-known result

$$\sigma_{\text{fus}}(E) = \pi R_b^2(1 - V_b/E), \quad (5)$$

where R_b and V_b are the radius and height of the Coulomb barrier for the s wave. For light nuclei, for which the number of partial waves is small, the last two assumptions may be very crude, as was noted in Ref. 22.

For below-barrier fusion of heavy ions, the classical representations (3) for the penetrabilities are no longer valid for calculations of penetration below the Coulomb barrier, and in this case the Wentzel–Kramers–Brillouin (WKB) approximation is used:

$$T_L(E) = 1/(1+t_L),$$

where

$$t_L = \exp 2\int_{r_1}^{r_2} [2\mu/\hbar^2]^{1/2}\,[V_L(r) - E]^{1/2}\, dr, \quad (6)$$

and the integration in this expression is between the turning points in the below-barrier region of the potential (1). We note that in the WKB approximation the penetrability does not depend on the behavior of the potential at distances at which $V(r) < E$, i.e., the reflection of the incident flux from regions of rapid variation of the potential is not taken into account.

Approximating the potential in the region of the Coulomb barrier by a parabola with curvature $\hbar\omega_L$:

$$\hbar\omega_L = \left|\frac{\hbar^2}{2\mu}\frac{d^2V_L}{dr^2}\right|^{1/2}_{r=R_{b_L}}, \quad (7)$$

Hill and Wheeler[23] obtained for t_L

$$t_L = \exp\left(2\pi\frac{V_{b_L} - E}{\hbar\omega_L}\right). \quad (8)$$

Assuming that the barrier curvature $\hbar\omega_L$ does not depend on L, and replacing the summation in (2) by an integration, Wong[24] was able to sum the series (2) and obtained

$$\sigma_{\text{fus}} = \frac{R_b^2\hbar\omega}{2E}\ln\left\{1 + \exp\left(2\pi\frac{E - V_b}{\hbar\omega}\right)\right\}. \quad (9)$$

At above-barrier energies, this expression reduces to (5). Wong was also able to obtain expressions for deformed nuclei by averaging (2) over the mutual orientations of the incident nucleus and the target nucleus.[24]

Equations (1)–(9) with the two free parameters V_b and R_b give a good description of the fusion cross section in the near-barrier energy range,[12] i.e., the fusion cross section σ_{fus} decreases linearly as a function of $1/E$ with typical parameter value $r_0 \approx 1.4$ F $[r_0 = R_b/(A_1^{1/3} + A_2^{1/3})]$. The standard optical model with an imaginary potential describing elastic scattering (and, therefore, the total reaction cross section)[25] gives for the strong-absorption radius a somewhat larger value[26]: $r_0 \simeq 1.5$ F. (The strong-absorption radius R_{SA} is defined as the distance of closest approach of two ions moving in a classical Rutherford orbit with angular momentum L for which the penetrability is $T_L = 0.5$.) This shows that direct processes are open at distances somewhat greater than the radius of the Coulomb barrier.

In considering the extent to which the above formalism can describe the experimental data, we begin with light nuclei.

Investigations of reactions with light nuclei, $^{12}C + {}^{12}C$, $^{12}C + {}^{16}O$, $^{16}O + {}^{16}O$, $^{16}O + {}^{9}Be$, etc., have two aims. On the one hand, the structure of light nuclei has been well studied, so that there is hope of obtaining reliable information about the reaction mechanism.

On the other hand, as we have already noted, below-barrier reactions with light nuclei are important for the understanding of processes in stars in the late stage of evolution, by which time nuclear reactions with hydrogen and helium have accumulated in the stars carbon and oxygen, whose burning at interaction energies $E \simeq 1$ MeV determines the evolution of the stars. From this point of view, extrapolation of the experimental data obtained at the present time in

the near-barrier region of energies up to several hundred kilo-electron-volts is very important.

For such an extrapolation we need a model with good physical foundation. To this end, experimental efforts have been devoted not only to measurement of these reactions but also to the extension of the investigations to the fusion cross sections of the neighboring nuclei.

Figure 1 shows the results of experimental studies with light nuclei, taken from the review of Ref. 27. In the measured range of energies, the cross sections decrease by five orders of magnitude, and for convenience they are therefore compared with the reaction cross section σ_{mod} calculated in the optical model with the parameter set $V = 50$ MeV, $W = 10$ MeV, $r_0 = 1.27$ F, and $\alpha = 0.4$ F.

The figure shows that the fusion cross section for the α-cluster carbon and oxygen nuclei exhibit a complicated resonance structure. Structures are found in the fusion cross sections for practically all reactions of α-cluster nuclei up to the fusion of two ^{28}Si nuclei and up to excitation energies of 70 MeV. A similar structure for these reactions is also found in the excitation functions in the total reaction cross section and in elastic and quasielastic scattering (see, for example, the review of Ref. 28). Nevertheless, the "smoothed" experimental fusion cross sections for all light nuclei do not differ strongly from the predictions of the standard optical model. At still lower energies, the fusion cross sections for the ^{16}O + ^{16,18}O reactions become smooth functions of the energy and can be described in the framework of one-dimensional models with a small renormalization of the standard parameters.[29] The differences in the cross sections for the different oxygen isotopes can be explained by the different geometrical sizes of the nuclei.

The agreement between the theoretical predictions and the experimental data at below-barrier energies is much poorer for reactions with intermediate nuclei. Figure 2 shows experimental data of Ref. 13 for the ^{58,64}Ni + ^{58,64}Ni reactions It can be seen that the addition of a few neutrons to the ^{58}Ni nucleus leads to a significant change of the slope in the fusion cross section for the ^{58}Ni + ^{64}Ni reaction. In addition, the energy shift between the fusion cross sections for the various nickel isotopes cannot be explained by a simple change in the geometrical sizes of the nuclei. A similar strong dependence of the fusion cross sections on the number of added neutrons is also found[30] in the ^{40}Ca + ^{40,44,48}Ca reactions with lighter nuclei. Figure 2 also shows the results of calculations in accordance with the Hill–Wheeler expressions (8) with a nucleus–nucleus potential obtained from the liquid-drop model.[31] It can be seen that in the low-energy part of the spectrum for the ^{58}Ni + ^{58}Ni reaction the calculated curve has the same slope as the experimental one but is shifted by 5 MeV to higher energies. For the ^{58}Ni + ^{64}Ni reaction, the slope of the theoretical cross section in the measured range of energies was found to be larger than the experimental slope. The discrepancy between theory and experiment increases still more as the mass numbers of the colliding ions are increased.[32]

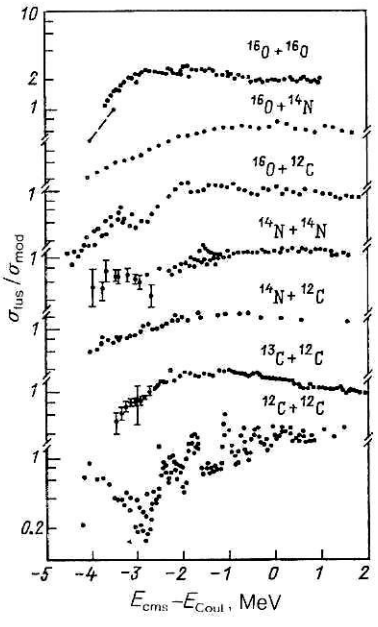

FIG. 1. Ratio of the cross sections of below-barrier fusion to the cross sections calculated in accordance with the optical model (from Ref. 27). The Coulomb energy was taken to be $Z_1 Z_2 e^2/R$, where $R = 1.7(A_1 A_1^{1/3} + A_2^{1/3})$.

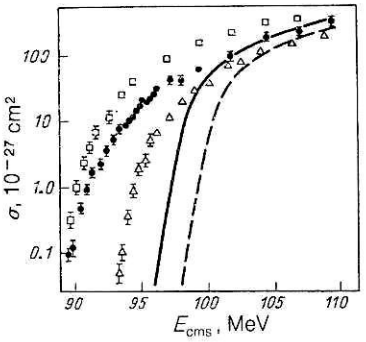

FIG. 2. Experimental cross sections for complete fusion for nickel isotopes[13]: open squares for ^{64}Ni + ^{64}Ni, black circles for ^{58}Ni + ^{64}Ni, and open triangles for ^{58}Ni + ^{58}Ni. The continuous and broken curves are WKB calculations for the ^{58}Ni + ^{64}Ni and ^{58}Ni + ^{58}Ni reactions, respectively.

A question that may be asked is this: What must be the height of the one-dimensional potential barrier if the data on below-barrier fusion are to be described satisfactorily? This inverse problem, analogous to that of the recovery in classical mechanics of the potential energy from the oscillation period, was solved in the semiclassical approximation in Ref. 33. Under certain simplifications, an expression was obtained for the difference $t(V) = r_2(V) - r_1(V)$ between the right and left turning points in the below-barrier region as compared with the known fusion cross section. The functions $r_2(V)$ and $r_1(V)$ themselves remain undetermined. In Ref. 33 it was assumed that the functional form of the potential at the right end of the barrier is given by the Coulomb potential and the tail of the nuclear liquid-drop potential,[31] and then the shape of the potential at the other end of the barrier was determined uniquely from the solution obtained to the inverse problem.

Examples of potentials recovered in this way for light and intermediate systems are given in Ref. 33. The potentials for the light systems, for example, ^{14}N + ^{14}N, do not exhibit significant deviations from the potentials usually employed.

For heavier nuclei, the potentials become very narrow

and even two-valued. Figure 3 reproduces a fragment of a figure in Ref. 33 for the recovered potentials in the fusion reactions $^{40}Ca + {}^{40}Ca \to F$, $^{64}Ni + {}^{64}Ni \to F$, and $^{64}Ni + {}^{74}Ge \to F$. The unexpected behavior of the potential can be explained in several ways. First, the expression for the inertial mass in the form $\mu = A_1 A_2 / (A_1 + A_2) M_n$ in the WKB penetrability (6) is valid only for light nuclei, in which the Coulomb barrier is situated at distances greater than the sum of the half-density radii of the two nuclei. For heavy nuclei, this is not the case, and the possibility of a distance dependence of the inertial parameter, i.e., $\mu \to M(r)$, was discussed in Ref. 32 in a description of the $^{64}Ni + {}^{74}Ge$ experiment. A phenomenological introduction of $\mu \to \mu/P$, where $P > 1$, was also used in the review of Ref. 27 to increase the WKB penetrability (6) in the description of experiments. Second, the one-dimensional description of the tunneling process is too crude for heavy nuclei, and other degrees of freedom must also be taken into account.

Systematic measurements of the cross sections of below-barrier fusion for intermediate nuclei were made in Ref. 34. Analysis of the experiment by means of Wong's expression (9) showed that the parameter $\hbar\omega$, which describes the curvature of the Coulomb barrier, increases with increasing masses of the nuclei that participate in the reaction and, for example, in reactions of argon with tin isotopes and of krypton with nickel isotopes, reaches values $\hbar\omega = 13$–16 MeV. It was noted in Ref. 34 that such curvature cannot be obtained even with a deep rectangular potential well, while the usually employed potentials give $\hbar\omega = 2$–4 MeV. We have already seen a similar sharp drop of the potential in the region of the inner edge of the Coulomb barrier in Fig. 3.

Thus, the first experiments on below-barrier fusion already presented difficult problems for theory. We shall now consider how additional information on the mechanism of complete fusion can be obtained from experiments at above-barrier energies.

On the transition to higher energies, $E \approx (2$–$3) V_b$, it was found that the fusion cross section becomes much less than the total reaction cross section, and that direct processes make an important contribution to the reaction cross section. Analysis of the experimental data showed[35] that in the high-energy region too a linear slope is observed in the fusion cross section as a function of $1/E$. At these energies, the fusion cross section is determined by the value and range

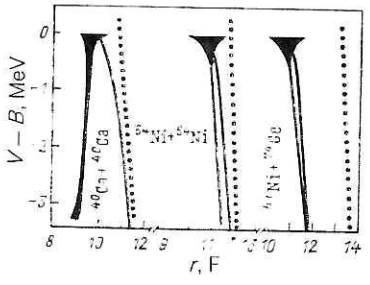

FIG. 3. Effective one-dimensional potential barriers recovered by solution of the inverse problem. The dotted lines are the Coulomb potentials of point charges Z_1 and Z_2. The black sections reflect the uncertainty in the barrier thickness due to the experimental errors in the measured fusion cross sections.

of the potential at a certain "critical" point with characteristic radial distance $r_{cr}^0 = 1 \pm 0.07$ F:

$$\sigma_{fus}(E) = \pi R_{cr}^2 (1 - V_{cr}/E), \tag{10}$$

and at these energies the expression (5) continues to describe the total reaction cross section. It was shown that for a large group of nuclei[35,36] a necessary condition for fusion at high energies is attainability for the heavy ions of the critical distance R_{cr} in the potential (1), while direct processes are open when the Coulomb barrier is attained.

Using this idea, Glas and Mosel[37] succeeded in summing the series (2), and they obtained a unified expression for the fusion cross section, valid at both high and low energies:

$$\sigma_{fus} = \frac{\hbar\omega R_b^2}{2E} \ln \frac{1 + \exp\{2\pi[E - V_b]/\hbar\omega\}}{1 + \exp\{2\pi[E - V_b - (R_{cr}/R_b)^2 (E - V_{cr})]/\hbar\omega\}} \tag{11}$$

The expressions (9) and (10) are obtained from (11) by going to the low- and high-energy limits, since for light and intermediate nuclei $V_b > V_{cr}$.

In the derivation of Eq. (11) it was assumed that the losses of kinetic energy at distances greater than R_{cr} are small. This question was investigated in Ref. 38 in the framework of the time-dependent Hartree–Fock method. It was shown that an appreciable discharge of kinetic energy into excitations occurs only at distances with radial parameter $r_0 \simeq 1$ F, corresponding to the sum of the half-density radii of the two nuclei. Here, the shell structures of the individual nuclei are rearranged into the single structure of the compound nucleus, and this clarifies the physical significance of the critical radius R_{cr} for fusion.

The expressions given above for the fusion cross sections are based on classical or semiclassical notions, which presuppose the existence in the above-barrier region of well-defined trajectories of the incident particle. A quantum-mechanical model for the description of fusion was constructed in Refs. 39–42. The essence of the model consists in the introduction, at distance $r = R_{cr}$, of a boundary condition on the wave function of the relative motion of the two ions in the form of just a converging wave. The flux of particles that reach the critical distance R_{cr} in the potential (1) determines the fusion cross section in this model. (For heavy ions similar boundary conditions, with a somewhat greater radial parameter $r_0 = 1.17$ F, were first introduced by Thomas in Ref. 43.) The multichannel variant of the model will be discussed in detail in the next section, and therefore we here make only brief comments.

In the initial variant of the model,[40,41] in the single-channel case, we introduced in the peripheral region of overlapping of the nuclei a phenomenological imaginary potential with energy dependence $W \sim W_0 (E - V_b)$ and $W = 0$ at below-barrier energies. In this model, the imaginary potential is responsible for the direct processes and ensures that the reaction cross section exceeds the fusion cross section at above-barrier energies. The model successfully describes the fusion cross sections and the total reaction cross sections at near-barrier and above-barrier energies for a large group of nuclei with a single set of parameters of the imaginary part of the potential.[41] Obviously, if the imaginary part is zero, the fusion cross section in this model can differ only little from

the cross section (11), and the difference is due to the quantum-mechanical description of the tunneling in the complicated potential (1).

Further, we pointed out that the imaginary potential used in Refs. 40 and 41 to describe fusion cross sections was too small to describe the differential cross sections for elastic scattering. But an increase of the imaginary potential to the usual value leads to a large decrease of the flux of particles from the ground-state channel, and the flux that reaches the critical distance and, therefore, the fusion cross section are too small. To resolve this contradiction, we introduced[44] a multichannel boundary-condition model, which permitted the system to pass from the ground-state channel to the inelastic channels at large radial distances. On the one hand, this ensured a correct description of the elastic scattering at near-barrier energies even without introduction of an imaginary part of the potential. On the other hand, part of the particle flux reached the critical distance in the inelastic channels and, therefore, contributed to the fusion cross section.

The contradiction in the description of elastic scattering and fusion was eliminated in a different way in Ref. 45, in which the authors separated the imaginary potential extracted from the elastic scattering into two parts: a peripheral part responsible for the direct processes, and a residual internal part that described the decrease of the flux entering the fusion channel. In this model, the partial fusion penetrabilities are determined by

$$T_L(E) = 8/\hbar v \int_0^{R_F} |\chi_L(r)|^2 W(r)\, dr, \qquad (12)$$

where v is the relative velocity of the two ions. The distorted partial waves $\chi(r)$ are calculated with the complete optical potential $V(r)$ and $iW(r)$, extracted from the elastic scattering, and this guarantees correct description of the elastic scattering phase shifts. Analysis of the experimental data on the fusion cross sections at above-barrier energies showed[45,46] that the upper limit of integration in the expression (12) is approximately constant and given by $R_F \approx 1.45(A_1^{1/3} + A_2^{1/3})$. However, in the below-barrier region of energies this one-dimensional model gave underestimations for the fusion cross section, and in subsequent studies the model was extended by the introduction of strong channel coupling in the peripheral region.[47]

Thus, having examined many one-dimensional models, we have shown that they are not capable of explaining the observed large cross sections of below-barrier fusion for intermediate nuclei, although they are very helpful for parametrization and systematization of the experimental data.[34]

2. MULTIDIMENSIONAL MODELS

Averaging over orientations and zero-point vibrations. Potentials

As soon as the unexpectedly large below-barrier fusion cross sections were discovered, attempts were made to explain them. When one of the colliding nuclei was deformed, the procedure of averaging the cross sections over the mutual orientations of the nuclei gave not only qualitatively but also quantitatively the necessary increase of the cross sections. We illustrate this by the example of Ref. 14, in which the spherical ^{16}O nucleus collided with the deformed nuclei ^{148,154}Sm.

In Ref. 24, Wong obtained approximate expressions for the averaged cross section in a deformed potential of Woods–Saxon type. In many cases, this potential is inconvenient, since it has three free parameters, known generally only approximately. The potentials most widely used today in heavy-ion physics are the double folding potential with M3Y forces,[48] the contact potential of Ref. 49, and the potential obtained in the energy-density formalism,[50] the parameters of which are fixed by the general properties of nuclear matter and the nucleon–nucleon interaction. A detailed discussion of the approximations made in the construction of ion–ion potentials can be found in Ref. 51. Here, we give a convenient parametrization of these potentials, which are the ones most often used in theoretical models and in the analysis of experiments and will be needed in the later exposition.

The nuclear part of the contact potential has the form[49]

$$V_{\text{nuc}}(r) = 4\pi\gamma \frac{C_1 C_2}{C_1 + C_2} \Phi(\zeta). \qquad (13)$$

Here, $\zeta = r - C_1 - C_2$ is the distance between the surfaces of the nuclei, $C_i = R_i - 1/R_i$ are the half-density radii of the nuclei, $R_i = 1.28A_i^{1/3} - 0.76 + 0.8A_i^{-1/3}$ are the radii of the nuclei in the droplet model,

$$\gamma = 0.9517\left[1 - 1.7826\left(\frac{N-Z}{A}\right)^2\right]$$

is the coefficient for the surface energy of the nuclei, and N, Z, and A are the numbers of neutrons, protons, and nucleons in the compound nucleus. The function $\varphi(\zeta)$ is parametrized in the form

$$\Phi(\zeta) = \begin{cases} -0.5(\zeta - 2.54)^2 - 0.0852(\zeta - 2.54)^3, & \zeta < 1.2511; \\ -3.437\exp(-\zeta/0.75), & \zeta > 1.2511. \end{cases}$$

The potential obtained in Ref. 50 has the even simpler form

$$Y_{\text{nuc}}(r) = \frac{A_1^{1/3}A_2^{1/3}}{A_1^{1/3} + A_2^{1/3}} U(s); \qquad (14)$$

$$s = r - r_0(A_1^{1/3} + A_2^{1/3});$$

$$U(s) = \begin{cases} -30\exp(-0.27\, s^2), & s > 0; \\ -30 + 6.3\, s^2, & s < 0 \end{cases},$$

and r_0 in this potential is varied in the range $r_0 = 1 \pm 0.07$ F. The procedure for averaging the cross sections for deformed nuclei, with an interaction described by these potentials, is as follows. We introduce the polar angle Θ, which specifies the orientation of the symmetry axis of the deformed target nucleus relative to the direction of the incident beam. Further, for axisymmetric nuclei we make the substitution

$$R_0 \to R_0\left[1 + \sum_\lambda \beta_\lambda Y_{\lambda 0}(\Theta)\right], \qquad (15)$$

where β_λ are the parameters of the static deformation of multipolarity λ. This expression is substituted in the analytic expressions for the potentials (or densities in the folding model), i.e., we successively transform the expressions (1), (6) or (8) and (2): $V_L(r) \to V_L(r, \Theta)$, $T_L(E) \to T_L(E, \Theta)$, and $\sigma_{\text{fus}}(E) \to \sigma_{\text{fus}}(E, \Theta)$. The result is obtained by integration:

$$\sigma_{\text{fus}}(E) = \int_0^{\pi/2} \sigma_{\text{fus}}(E, \Theta) \sin\Theta \, d\Theta. \quad (16)$$

Figure 4 shows such an analysis of the experimental data for the $^{16}O + {}^{148,154}Sm$ reactions.[52] The first target nucleus is practically spherical, but the second is strongly deformed. The figure shows the sensitivity of the below-barrier fusion cross section to the parameters of the static quadrupole deformation of the target nucleus. The deformation parameters extracted from this experiment for the ^{148}Sm nucleus were found to be somewhat higher than the values usually adopted. It should be noted that an equally good description of the experiment is also obtained by introducing a parameter $P > 1$ for the renormalization of the effective mass. It was also shown in Ref. 53 that this experiment can also be described under different assumptions, for example, by assuming that the ^{154}Sm nucleus is spherical and setting the parameter $\hbar\omega = 8.5$ MeV in Wong's formula (9).

Allowance for negative hexadecapole deformation of the target nucleus also leads to a similar enhancement of the below-barrier fusion cross section. Test calculations[54] for the $^{16}O + {}^{184}W \to F$ reaction showed that the greatest increase of the fusion cross section is obtained when the quadrupole and negative hexadecapole deformations are taken into account simultaneously.

We see that by choosing the parameters of the phenomenological models in different ways we can obtain equally good descriptions of the below-barrier fusion cross sections for deformed nuclei. Therefore, to test the various models it is necessary to measure other quantities too that characterize the decay of the compound nucleus.

We turn to spherical nuclei, for which a procedure for averaging over the zero-point vibrations of the surfaces of the colliding nuclei was proposed.[55] By analogy with the deformed nuclei, we can specify a distribution of the nuclear radii,

$$R = R_0 \left\{1 + \sum_{n\lambda\mu} \alpha_{n\lambda\mu} Y_{\lambda\mu}(\Theta)\right\}, \quad (17)$$

where $\alpha_{n\lambda\mu}$ are the dynamical-deformation parameters of the target nucleus. Assuming independent harmonic vibrators for each vibration mode, we obtain for the distribution function of the nuclear radii in the ground state

$$g(R) = \left\langle 0 \left| \delta\left(R - R_0\left(1 + \sum_{n\lambda\mu} \alpha_{n\lambda\mu} Y_{\lambda\mu}\right)\right) \right| 0 \right\rangle = (2\pi\sigma^2)^{-1/2} \exp\left(-\frac{(R-R_0)^2}{2\sigma^2}\right), \quad (18)$$

where the variance of the distribution can be expressed in terms of the mass parameter $D_{n\lambda}$ of the collective nuclear model and the energy $\omega_{n\lambda}$,[56]

$$\sigma^2 = R_0^2 \sum_{n\lambda} \frac{2\lambda+1}{4\pi} \frac{\hbar}{2D_{n\lambda}\omega_{n\lambda}} = \sum_{n\lambda} \sigma_{n\lambda}^2, \quad (19)$$

or in terms of the reduced probability of electromagnetic transitions, expressed in single-particle units:

$$\sigma_{n\lambda} = \frac{R_0}{Z(\lambda+3)} [(2\lambda+1) B(E\lambda)_{\text{Wu}}]^{1/2}.$$

For the quadrupole and octupole vibrations, which make the greatest contribution on account of their high collectivization, this reduces to

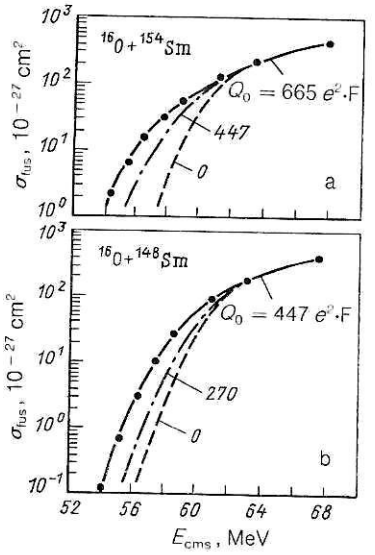

FIG. 4. Below-barrier fusion cross sections for the reactions $^{16}O + {}^{154}Sm$ (a) and $^{16}O + {}^{148}Sm$ (b) as functions of the collision energy and with different quadrupole moments of the ^{154}Sm nucleus.

$$\sigma_\lambda = R_0 \beta_\lambda / (4\pi)^{1/2}, \quad (20)$$

where β_λ is a dynamical-deformation parameter that can be extracted from independent experiments.[56] When the dynamical vibrations of both nuclei are taken into account, the summation in (19) is also extended to the second nucleus.

In this procedure, the fusion cross section is calculated as follows. The potential in the expression (1) becomes dependent on the dynamical variable s, i.e., $V(r) \to V(r - R_0 - s)$. The partial penetrability $T_L(E, s)$ is then averaged with the weight function (18):

$$T_L(E) = \int_{-\infty}^{\infty} g(s) T_L(E, s) \, ds. \quad (21)$$

In practical calculations, the integration is usually evaluated within the range of three standard deviations σ, and the penetrabilities are calculated in accordance with the Hill–Wheeler expression (8) for $T_L > 0.45$ and the WKB expression (6) at lower values.

It is natural to ask how the convergence of the cross sections (16) and (21) depends on the number of levels taken into account. In the procedures for averaging over the orientations and the zero-point vibrations, it is assumed that the nuclei maintain their orientation or shape during the time τ of their passage below the Coulomb barrier, i.e., the rotation energy or vibration energy must not be large, $\varepsilon < \hbar/\tau$. Estimates of the "imaginary time" of tunneling below a parabolic barrier with curvature $\hbar\omega$ give[16]

$$\tau = \int \frac{dr}{\{2\mu[V(r) - E]\}^{1/2}} \approx \frac{\pi}{\omega}.$$

For the standard potentials, as we have already noted, $\hbar\omega = 2$–4 MeV, i.e., only the low-lying collective states can contribute to the enhancement of the below-barrier fusion, and the summation in (15) and (19) can be limited by the condition $\varepsilon < \hbar\omega/\pi$.

The procedure described above was used to calculate below-barrier fusion cross sections for a large group of spherical nuclei.[17,57–59] It was found that the parameters σ

extracted from the experimental data on below-barrier fusion were well correlated with the $B(E\lambda)$ values extracted, for example, from the scattering of electrons and fast protons, Coulomb excitation, and other independent experiments. However, there were exceptions, in the form of both excesses and shortfalls of the experimental values; these were subsequently explained on the basis of multichannel models.

Boundary-condition model

It was shown in Refs. 16, 17, and 60 that both procedures of averaging for spherical and deformed nuclei are special cases of a more general approach based on allowance for the strong channel coupling in the peripheral region and the strong absorption within a nucleus at a distance with characteristic parameter $r_0 \approx 1$ F, which is typical of the description of fusion cross sections at high energies.[35-38]

Strong absorption can be introduced by boundary conditions in the form of just a converging wave or by a soft imaginary part of the potential with depth $W = 10$ MeV and radial form factor in the form of the square of the Woods–Saxon potential with parameters $r_0 = 1$ F and $a = 0.4$ F, as was done in Ref. 61. (It is necessary to choose the depth of the imaginary part with care, since it was shown in Ref. 62 that a very large depth leads to reflection of the incident flux, and not to strong absorption, as one might have expected intuitively.)

On the basis of Ref. 21 we briefly review the most important assumptions in the derivation of the expressions for the differential cross sections for elastic and inelastic scattering and for fusion and reaction cross sections.

We choose the Hamiltonian of the system that describes the interaction of the two nuclei in the form

$$H = T + H_0(\xi) + V(r, \xi). \tag{22}$$

Here, T is the kinetic-energy operator, V is the operator of the interaction of the two nuclei, which depends on the relative distance r and on the internal coordinates ξ, and H_0 is the internal Hamiltonian of the target nucleus (to simplify the exposition, we ignore the internal structure of the incident ion, and we set the spin of the target equal to zero).

Expanding the wave function of the total Hamiltonian in a series with respect to the eigenfunctions of the internal Hamiltonian, $H_0\varphi_\alpha = \varepsilon_\alpha \varphi_\alpha$, and then with respect to partial waves, we obtain the well-known system of equations of the method of strong channel coupling[60] for the radial wave functions $R_{\alpha L_\alpha}(r)$, that describe the relative motion of the two ions:

$$\left[\frac{d^2}{dr^2} + \frac{2\mu}{\hbar^2}(E - \varepsilon_\alpha - V_\alpha(r)) - \frac{L_\alpha(L_\alpha+1)}{r^2}\right] R_{\alpha L_\alpha}(r) = \frac{2\mu}{\hbar^2}\sum_\beta V_{\alpha\beta}(r) R_{\beta L_\beta}(r). \tag{23}$$

Here, L_α is the orbital angular momentum, $V_\alpha(r)$ is the diagonal part of the interaction potential of the two nuclei in channel α,

$$V_\alpha(r) = \langle \varphi_\alpha \mid V(r, \xi) \mid \varphi_\alpha \rangle, \tag{24}$$

and $V_{\alpha\beta}(r)$ is the potential of the coupling between the ground-state channel and the excited channels:

$$V_{\alpha\beta}(r) = \langle \varphi_\alpha \mid V(r, \xi) \mid \varphi_\beta \rangle. \tag{25}$$

On the radial wave functions $R_{\alpha L_\alpha}$ the usual boundary conditions are imposed at large distances:

$$R_{\alpha L_\alpha}(r) = [G_{L_\alpha}(x) - iF_{L_\alpha}(x)]\,\delta_{\alpha\alpha_0} - S^{L_\alpha}_{\alpha\alpha_0}[G_{L_\alpha}(x) + iF_{L_\alpha}(x)], \tag{26}$$

where the argument of the regular, $F_L(x)$, and irregular, $G_L(x)$, Coulomb functions is $x = k_\alpha r$. (As usual, the channel with index zero corresponds to the ground state of the target nucleus.)

In the traditional method of strong channel coupling, the conditions of regularity of the wave functions at the origin, i.e., $R_{\alpha L_\alpha}(0) = 0$, are used to provide the second boundary condition. In each channel we impose on the wave functions of the relative motion a condition that there be just a converging wave at distance $r = R_{cr}$. For this purpose boundary conditions of WKB type were used in Ref. 15:

$$R_{\alpha L_\alpha}(r \approx R_{cr}) = A_{\alpha L_\alpha} \frac{\sqrt{k_\alpha}}{\sqrt{k^1_{\alpha L_\alpha}(r)}} \exp\left[-i\int_{R_{cr}}^{r} k^1_{\alpha L_\alpha}(r')\,dr'\right], \tag{27}$$

where $k^1_{\alpha L_\alpha}$ is the local wave number in channel α,

$$k^1_{\alpha L_\alpha}(r) = k_\alpha(1 - V_L(r)/(E - \varepsilon_\alpha))^{1/2}, \tag{28}$$

and $k_\alpha = (2\mu(E - \varepsilon_\alpha)/\hbar^2)^{1/2}$ is the asymptotic wave number.

In Refs. 21 and 39–41 we used as boundary conditions Hankel functions of the second kind:

$$R_{\alpha L_\alpha}(r = R_{cr}) = A_{\alpha L_\alpha} \hbar^{(2)}_{L_\alpha}[k^1_{\alpha L_\alpha = 0}(R_{cr})\, R_{cr}]. \tag{29}$$

Hankel functions solve the Schrödinger equation in the potential of a rectangular well exactly. For light ions, approximation of the central potential by a rectangular well at $r = R_{cr}$ is justified, since the smallness of the Coulomb potential means that the total potential is negative and has a minimum near R_{cr}. The negative sign of the potential also ensures fulfillment of the condition $L \ll k^1_\alpha(R_{cr})R_{cr}$, which is needed if the Hankel functions are to represent converging waves.

Boundary conditions of a different type in the form of convergent waves for exponentially decreasing potentials were constructed in Ref. 64 and used to describe heavy-ion elastic scattering.

Equations (22)–(25) are given in a form suitable for describing coupling to the channels of inelastic excitation of rotational or vibrational levels. However, transfer reactions can also be included in the general scheme if recoil effects are ignored. We shall see that the channels of few-nucleon transfers and of inelastic excitation make equally important contributions to the enhancement of the below-barrier fusion.

Solution of the system of Schrödinger equations with the boundary conditions (26) and (27) or (29) permits determination of the coefficients $A_{\alpha L_\alpha}$ and the elements of the S matrix in the elastic, $\alpha = 0$, and inelastic channels, which determine the cross sections of all the processes in which we are interested.

The fluxes of particles that reach the distance $r = R_{cr}$ can be calculated by means of the wave fucntions (27) or (29). In the considered model, they determine the fusion cross section in channel α,

$$\sigma_{\text{fus}} = \frac{\pi}{k_0^2} \sum_L (2L+1) \mid A_{\alpha L_\alpha} \mid^2 \frac{k_\alpha}{k_0}, \tag{30}$$

and the total fusion cross section

$$\sigma_{\text{fus}} = \sum_\alpha \sigma_{\text{fus}}^\alpha. \tag{31}$$

The elements of the S matrix in the elastic and inelastic channels determine the differential cross sections for elastic and inelastic scattering in the usual manner:

$$\frac{d\sigma_{\text{el}}(\Theta)}{d\Omega} = \Big| f_{\text{Coul}}(\Theta) + \frac{i}{2k_0} \sum_L (2L+1) \times e^{2i\sigma_L} (1 - S^L_{\alpha_0\alpha_0}) P_L(\cos\Theta) \Big|^2; \tag{32}$$

$$\frac{d\sigma^\alpha_{\text{inel}}(\Theta)}{d\Omega} = \frac{\pi}{k^2} \sum_M \Big| \sum_{LL_0} (2L_0+1)^{1/2} \langle LM\lambda - M \mid L_0 0\rangle\, i^{L_0 - L} e^{i(\sigma_L + \sigma_{L_0})} * S^L_{\alpha\alpha_0} Y_{LM}(\Theta) \Big|^2 \frac{k_\alpha}{k_0}; \tag{33}$$

they also determine the total cross section in the inelastic channel α,

$$\sigma^\alpha_{\text{inel}} = \frac{\pi}{k_0^2} \sum_{l\,L_0} (2L+1) \mid S^L_{\alpha\alpha_0} \mid^2 \frac{k_\alpha}{k_0}, \tag{34}$$

and the total reaction cross section

$$\sigma_r = \frac{\pi}{k_0^2} \sum_L (2L+1)(1 - \mid S^L_{\alpha_0\alpha_0} \mid^2). \tag{35}$$

The coupling potentials that occur in (23) are real, and therefore the total particle flux is conserved, and the unitarity relation holds for the cross sections: $\sigma_r = \sigma_{\text{inel}} + \sigma_{\text{fus}}$. In models in which the absorption is introduced by an imaginary potential within the nucleus,[18,61] this condition permits determination of the fusion cross section as the difference $\sigma_{\text{fus}} = \sigma_r - \sigma_{\text{inel}}$ and the use for calculations of σ_r and σ_{inel} of the standard programs of the method of strong channel coupling that have been developed to describe inelastic excitations.

To make numerical calculations, we must particularize the potentials that occur in the system of equations (23). In the channel-coupling potential (25), we separate the angular variables[63]:

$$V_{\alpha\beta}(r) = \frac{(2L_\beta+1)^{1/2}}{(4\pi)^{1/2}(2\lambda+1)^{1/2}} (-1)^{L_\alpha - \lambda} \langle L_\alpha 0 L_\beta 0 \mid \lambda 0\rangle F_\lambda(r), \tag{36}$$

where λ is the spin of the excited level, and $F_\lambda(r)$ is the radial form factor of the transition. For the excitation of low-lying collective states of nuclei, which will be considered in this work, we shall use the standard expression[56] of the macroscopic model for the form factor of the potential of the coupling between the ground-state channel and the excited channels:

$$F_\lambda(r) = \beta_\alpha R_0 \frac{dV_{\text{nuc}}(r)}{dr} + \frac{3}{2\lambda+1} \beta_\alpha R_c Z_1 Z_2 e^2 \begin{cases} R_c^{\lambda-1}/r^{\lambda+1}, & r > R_c \\ r^\lambda / R_c^{\lambda+2}, & r < R_c \end{cases}, \tag{37}$$

where β_α is the dynamical-deformation parameter for excitation of level α, R_0 is the radius of the nucleus, and R_c is the charge radius. The second term in this expression describes Coulomb excitation. To reduce the number of parameters, it is usually assumed that $R_c = R_0$.

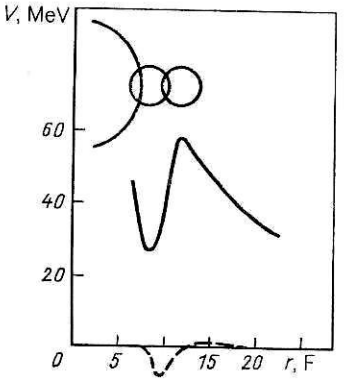

FIG. 5. Central potential (continuous curve) and coupling potential (broken curve) as functions of the distance between the centers of the ^{14}C and ^{208}Pb nuclei. The configurations of the nuclei for $r = R_{cr}$ and $r = R_b$ are shown at the top.

The form factors of the nuclear and Coulomb excitations have opposite signs, and they do not completely cancel at $r = R_{cr}$. To avoid a jump of the coupling potential at the point $r = R_{cr}$, which reflects the flux, we introduce a factor, by which we multiply the coupling form factor (37):

$$P = 1 - \exp\left[-\left(\frac{r - R_{cr}}{a_p} \right)^2 \right], \tag{38}$$

where a_p is a small quantity (in the calculations, we used throughout $a_p = 0.3$ F). Mathematically, this means that in the system of equations (23) the channels are decoupled from each other at $r = R_{cr}$. Calculations showed that the introduction of this factor results in a small redistribution of the incident flux between the channels without changing the total fusion cross section.

As an illustration, Fig. 5 shows the central potential and coupling potential for the 3^- level for $^{14}C + ^{208}Pb$. The upper part of the figure shows the positions of the half-density radii C_i in the potential (13) at $r = R_{cr}$ and $r = R_b$. It can be seen that already at $r = R_{cr}$ the nuclei are effectively separated. Thus, the assumption that the tunneling in the model is

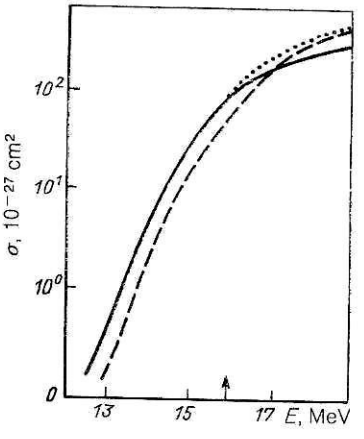

FIG. 6. Fusion cross section (continuous curve) and reaction cross section (dotted curve) for $^{16}O + ^{27}Al$ as functions of the c.m. energy of the incident ion. The broken curve is the calculation without channel coupling. The arrow shows the height of the Coulomb barrier.

determined by the spectrum of separated nuclei is justified for light and intermediate nuclei.

In Fig. 6, for the $^{16}O + {}^{27}Al$ reaction, we represent a typical calculation of the reaction and fusion cross sections with allowance for only nuclear excitation of one level in the ^{27}Al nucleus with parameters $\lambda = 2, \beta R_0 = 1$ F, $\varepsilon = 1$ MeV. It is not important to take into account the Coulomb excitation for these nuclei. The parametrization (14) was used for the nuclear part of the central potential.

It can be seen from the figure that in the region of below-barrier energies allowance for channel coupling leads to a shift of the fusion cross-section curve to lower energies with virtually no change of its slope.

We note that coupling to the inelastic excitation channels at energies above the Coulomb barrier leads to a decrease of the fusion cross section compared with the one-dimensional model. For this reason, the nuclear potentials that describe the fusion cross sections at near-barrier energies in the one-dimensional models[12] must be changed in order to reduce the height of the Coulomb barrier. This must lead to an even greater increase of the below-barrier fusion cross section.

The total reaction cross section is practically equal to the fusion cross section at below-barrier energies. Above the Coulomb barrier, with increasing energy of the incident ion, the reaction cross section begins to grow faster than the fusion cross section, owing to the growth in the cross section for the inelastic processes. Increase of the coupling potential in the above-barrier case results in a rapid increase of the inelastic cross section, and the reaction cross section also grows rapidly, while the fusion cross section decreases slowly.[44] Thus, the parameters of the considered model determine a large group of quantities that can be measured at energies near the height of the Coulomb barrier, and they can be determined from independent experiments.

Special cases of decoupling of the equations

For a qualitative understanding of the reason for the increase in the below-barrier fusion cross section, we make some model simplifications. We consider a two-level system with zero excitation energy and zero spin. In this case, the system of equations (23) is decoupled by the ansatz[65]

$$\chi_L^{(\pm)}(r) = R_{0L}(r) \pm R_{1L}(r).$$

Using the obvious equations $V_0(r) = V_1(r)$ and $V_{01}(r) = V_{10}(r)$, we obtain for the functions $\chi_L^{(\pm)}(r)$ the equation

$$\left[\frac{\hbar^2}{2\mu}\frac{d^2}{dr^2} + E - \frac{L(L+1)\hbar^2}{2\mu r^2} - (V_0(r) \pm V_{01}(r))\right]\chi_L^{(\pm)}(r) = 0.$$

It can be seen from these equations that, irrespective of the sign of the coupling potential, there exists a channel in which the Coulomb barrier is effectively decreased. It is this circumstance, as we shall see in what follows, that is the reason for the increase in the below-barrier fusion cross section even when allowance is made for the loss of energy on internal excitations.

From the last equation we can obtain an expression for the fusion cross section. We shall assume that the potential $V_{01}(r)$ does not change the curvature and radius of the Coulomb barrier. Using in this case Wong's expression (9) for the below-barrier penetrability in the channels with wave functions $\chi_L^{(+)}$ and $\chi_L^{(-)}$, and using the condition of conservation of the total particle flux, we obtain[66]

$$\sigma_{\text{fus}} = \frac{\hbar\omega R_b^2}{4E}\left\{\ln\left[1 + \exp\frac{2\pi}{\hbar\omega}(E - V_0(R_b) - V_{01}(R_b))\right] + \ln\left[1 + \exp\frac{2\pi}{\hbar\omega}(E - V_0(R_b) + V_{01}(R_b))\right]\right\}. \tag{39}$$

For $E \gg V_0(R_b) + |V_{01}(R_b)|$ this expression is identical to (5). When $E < V_0(R_b) + |V_{01}(R_b)|$, the expression (39) can be simplified still further. Retaining only one term in the brackets and expanding the logarithm in a series, we obtain

$$\sigma_{\text{fus}}(E) = \delta\sigma_{\text{fus}}^0(E),$$

where $\sigma_{\text{fus}}^0(E)$ is the cross section without allowance for the channel coupling, and δ is an enhancement coefficient:

$$\delta = \exp\left[\frac{2\pi}{\hbar\omega}|V_{01}(R_b)| - \ln 2\right]. \tag{40}$$

It can be seen from this expression that the energy shift of the fusion cross section is determined by the coupling potential at distances near the Coulomb barrier.

At the barrier, the coupling potential (36) can be estimated by the following arguments.[66] At the barrier, the derivatives of the nuclear and Coulomb potentials are equal: $dV_{\text{nuc}}(r = R_b)/dr = Z_1 Z_2 e^2 / R_b^2$, and, taking into account the quadrupole Coulomb interaction, we have

$$V_{\text{fus}}(R) = \frac{\beta R Z_1 Z_2 e^2}{(4\pi)^{1/2} R_b^2}\left[1 - \frac{3}{5}\frac{R}{R_b}\right] \approx \frac{\beta R V_b}{(4\pi)^{1/2} R_b}\left[1 - \frac{3}{5}\frac{R}{R_b}\right]. \tag{41}$$

This expression shows that the shift of the curve for the fusion cross section to lower energies is determined not only by the collectivization βR of the state but also by the factor V_b / R_b, which increases rapidly on the transition to heavy nuclei. The second term in the brackets (the Coulomb excitation) reduces the coupling strength, and for symmetric systems, for which $R / R_b \approx 0.5$, it is 30%, while for asymmetric systems it is 60%. Thus, we now understand why the experimental data on the below-barrier fusion cross sections for light nuclei[27,29] can be described by a small renormalization of the parameters of the standard potentials.

As we see, the method of strong channel coupling with total absorption of the particles in the interior region of the nucleus is a good basis for describing processes of below-barrier tunneling. Unfortunately, realistic calculations of the effects of the channel coupling require much time and are complicated. Efforts were made to reduce the number of channels and apply faster algorithms to solve the system of coupled equations (23).

It was shown numerically in Ref. 67 that the effect of the coupling to the vibrational states of various multipolarities can be well reproduced if it is assumed that all excitations are monopole. This greatly reduces the number of possible subchannels possessing total angular momentum J and differing only in the orbital angular momentum. Indeed, if we ignore the angular-momentum transfer in inelastic excitations, we can show that all the coupling potentials for the

subchannels with energy ε and multipolarity λ have the same radial dependence and differ only in the Clebsch–Gordan coefficient. For these subchannels, we can introduce a single common function[68]

$$\overline{\Psi} = (N_1\Psi_1 + \ldots + N_n\Psi_n)/N, \tag{42}$$

where N_i are the numerical factors in front of the radial form factor (36), and $N = (\Sigma_i^2)^{1/2} = 1/\sqrt{4\pi}$ from the properties of the Clebsch–Gordan coefficients. In this case, the channel with the wave function (42), which "effectively" takes into account all the subchannels of the level with multipolarity λ, is coupled to the ground state by the form factor $F(r)/\sqrt{4\pi}$, which no longer depends on the orbital angular momentum.

For the solution of the system of coupled differential equations of second order iterative methods[69,70] have proved to be very effective, but they require great computational efforts. For qualitative estimates of the importance of the various channels, numerous simplifications for approximate solution of the system (23) have been proposed.

The system (23) can be decoupled if all the channels are degenerate and all the coupling potentials have the same form factor, i.e., $\langle\alpha|V|\beta\rangle = F(r)W_{\alpha\beta}$. Then there exists a matrix $U_{\gamma\delta}$ that diagonalizes the matrix W_β:

$$\sum_{lk} U_{nl}W_{lk}U_{km}^{-1} = \lambda_m\delta_{mn} \tag{43}$$

with eigenvalues λ_m, and this matrix realizes the decoupling,

$$\chi_\alpha(r) = \sum_\beta U_{\beta\alpha}R_\beta(r). \tag{44}$$

From the condition of conservation of the total particle flux, we obtain for the total penetrability

$$T = \sum_m |U_{m0}|\, T(E, V(r) + \lambda_m). \tag{45}$$

The procedures described above for averaging the cross sections over the orientations for deformed nuclei and over the zero-point vibrations for spherical nuclei can, as was shown in Refs. 16, 17, and 60, be obtained directly from this expression.

The system of equations (23) can also be decoupled in the more general case of several channels and without neglect of the excitation energy (60). However, in this case it is necessary to assume that the coupling potentials are constant within the Coulomb barrier, i.e.,

$$\varepsilon_\alpha\delta_{\alpha\beta} + \langle\alpha|V|\beta\rangle = M_{\alpha\beta}, \tag{46}$$

and then proceed by analogy with the preceding case, performing the transformations (43)–(45) successively. We describe in more detail the case when only one excited channel, with excitation energy ε and with constant strength F of the coupling to the ground-state channel, is taken into account. The eigenvalues of the matrix $M_{\alpha\beta}$ are

$$\lambda_\pm = [\varepsilon \pm (\varepsilon^2 + 4F^2)^{1/2}]/2 \tag{47}$$

and the weight factors are

$$U_\pm^2 = F^2/[F^2 + \lambda_\pm^2]. \tag{48}$$

It was shown in Ref. 67 that approximate allowance of this kind for the coupling somewhat overestimates the fusion cross section compared with the exact allowance in the method of strong channel coupling, but its simplicity is convenient for making estimates.

One further version of diagonalization of the interaction matrix was considered. In Ref. 71, the coupling matrix (46) was not assumed to be constant and was diagonalized by a unitary transformation $U_{\alpha\beta}(r)$ with dependence on the separation of the ions. Assuming in the below-barrier case that the tunneling occurs only in one channel, with the minimal eigenvalue $\lambda(r)$, we obtain the "effective adiabatic potential"

$$\zeta(r) = V_0(r) + \lambda(r), \tag{49}$$

in which the correction $\lambda(r)$ takes into account the contribution of the remaining channels to the probability of tunneling in the ground-state channel. When allowance is made for only one excited level, the eigenvalue $\lambda(r)$ can be determined from the expression (47), but now with a potential $F(r)$ that depends on the distance r. From Fig. 5 and the expressions (47) and (49) it can be seen that the renormalization leads to a reduction of the central potential within the nucleus due to the nuclear coupling potential and, outside the nucleus, due to the Coulomb excitation potential. This increases the curvature $\hbar\omega$ of the central potential, and in accordance with (41) the change in the curvature increases with increasing charges of the colliding ions. Thus, the phenomenologically found increase in the barrier curvature[34] finds a qualitative explanation in the framework of the model.

Convergence of the solutions

We now consider how the convergence of the solutions depends on the number of levels taken into account. Test calculations,[21] and also estimates made in Ref. 60, showed that with increasing excitation energy the coefficient of the increase in the fusion cross section is proportional to

$$\exp \sum_\alpha \beta_\alpha^2/\varepsilon_\alpha.$$

It can be expected that for transitions to vibrational states of spherical nuclei this series converges rapidly, since the majorizing series $\Sigma\beta_\alpha^2\varepsilon_\alpha$ for fixed multipolarity is proportional to the well-known energy-weighted sum rule, and the number of possible multipoles for collective transitions is limited by the size of the nucleus. Direct transitions to states with more complicated structure must be suppressed by the large difference between the wave functions of the initial and final states.

In Fig. 7 we give the results of calculations[72] by the method of strong channel coupling for the ^{50}Ti + ^{90}Zr reaction. It can be seen that allowance for the lowest collective 2^+ state significantly improves the agreement with the experimental data in comparison with the WKB case but still underestimates the cross section at low energies. Assuming that the excited states of the nuclei are pure vibrators, we obtain a correct description at low energies by taking into account the six lowest states. Allowance for these states by the method of averaging over the zero-point vibrations [see Eqs. (17)–(21)] overestimates the fusion cross section at low energies, owing to the neglect of the excitation energy.

Coupling to few-nucleon transfer channels

Hitherto, we have considered the channels of only inelastic excitation of the colliding nuclei, and in most cases

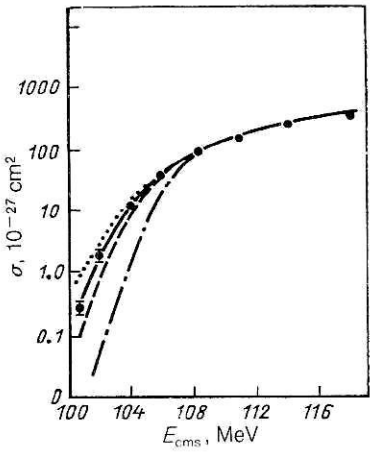

FIG. 7. Fusion cross sections for the $^{50}Ti + {}^{90}Zr$ reaction (from Ref. 72). The continuous and broken curves are coupled-channel calculations with six and two levels, respectively; the chain curve is the WKB calculation, and the dotted curve is with allowance for excitations in the method with zero-point vibrations.

this has been sufficient for correct description of the experimental data.[32] However, for some reactions other channels must also be taken into account. To explain the enhancement of the below-barrier fusion cross section in the $^{58}Ni + {}^{64}Ni$ reaction as compared with the $^{58}Ni + {}^{58}Ni$ reaction, it was noted in Refs. 73 and 74 that it is important to take into account the channel with transfer of two neutrons from the ^{64}Ni nucleus to ^{58}Ni. This channel has a positive value of Q_{react}, which is determined by the difference of the masses of the nuclei in the channel with rearrangement of the particles and entrance channel. In this case, some of the internal energy of the incident ions can go over into energy of the relative motion (for inelastic excitation reactions, $Q = -\varepsilon$). Besides this, in the process of rearrangement of the nuclei there is a change of the central potential due to the change of the geometrical sizes and of the charges of the incident ions. Thus, the central potential $U_0(r)$ in the channel with rearrangement of the particles is changed by

$$Q_{\text{eff}} = Q_{\text{react}} + \Delta E_{\text{Coul}}, \tag{50}$$

where ΔE_{Coul} is the difference between the heights of the Coulomb barriers for the two channels. For the two-neutron transfer channel in the $^{58}Ni + {}^{64}Ni$ reaction, estimates give $Q_{\text{eff}} = 3.9$ MeV. It was found[73] that 6% of the probability of transition of this system to the channel with transfer of two neutrons ensures a good description of the experimental data shown in Fig. 2.

The influence of the inelastic-excitation channels and the single-nucleon transfer channels on elastic scattering and fusion in the $^{16}O + {}^{208}Pb$ reaction at near-barrier energies was investigated in Ref. 75; four vibrational channels and eight transfer channels were taken into account, a good description of the data was obtained, and it was shown that allowance for vibrations alone is inadequate.

The few-nucleon transfer cross sections were measured at below-barrier energies in Ref. 76 for reactions of $^{16,18}O$ and ^{58}Ni with various tin isotopes. In these reactions there exist channels with positive Q_{react}, but enhancement of the below-barrier fusion cross sections in comparison with the one-dimensional models was observed only in the reactions with nickel ions. At the same time, correlations in the cross section of single-nucleon transfers for various tin isotopes with the enhancement of the fusion cross section for the same nuclei were found. We note that for the tin isotopes the probabilities of electromagnetic transitions and the level energies change little in going from one nucleus to another, and therefore the enhancement of the fusion cross section associated with the inelastic channel is approximately the same for them. In Ref. 77, it was found for the $^{58}Ni + {}^{64}Ni$ reaction that the cross sections of two-nucleon transfers go with excitation of levels with an energy around 4 MeV, so that the "effective" Q_{react} becomes negative. Thus, it may be concluded[76] that the enhancement of the below-barrier fusion cross sections due to the coupling to the transfer channels is related to the mean value of the transfer cross section and not to a positive value of Q_{react} for some particular channel.

In Ref. 78, the coupled-channel method was used to describe the below-barrier fusion cross sections in the $^{28,30}Si + {}^{58,62,64}Ni$ reactions with allowance for the inelastic excitation channels and single- and two-nucleon transfers. The influence of the shape of the radial form factors of the strength of the coupling of the various channels on the enhancement of the fusion cross sections and the cross sections of quasielastic processes was investigated. The diffuseness of the coupling potential of Woods–Saxon type was taken for single-nucleon transfer reactions to be twice as large as for inelastic excitation and the two-nucleon transfer channel. Thus, the form factor of the single-nucleon transfers had a long tail, stretching far beyond the Coulomb barrier, and this ensured a large cross section for the single-nucleon transfers. But the contribution of these processes to the enhancement of the below-barrier fusion cross section was small, since the strength of the coupling for these processes to the ground-state channel in the region of the Coulomb barrier is small. This shows that the enhancement of the fusion due to a particular level is not necessarily correlated with the excitation cross section of the level. We note that this result depends on the radial shape of the employed form factors, and therefore the problem of choosing the correct shape of the form factor for heavy nuclei in the interior region of the nuclei is very topical.

Reduction to one-dimensional equations. Polarization potential

The complexity of the solution of the multichannel system of equations led many authors to attempt the construction of a dynamical polarization potential that takes into account "effectively" the effect of coupling to other channels on the motion of the system in the ground-state channel.[79,80] In Ref. 81, this aim was achieved by approximate separation of the variables that describe the relative and internal motions and the coupling between them, and by the derivation of an effective Hamiltonian. The upshot was a radial Schrödinger equation with renormalized reduced mass, renormalized potential, and collective parameters of the nuclei.[81] Having in mind the results of solution of the inverse problem[33] (see Fig. 3), we consider two cases: a change in the shape of the potential barrier on the right due to allowance for the coupling of the relative motion to the low-lying collective excitations in nuclei[82] and influence of the nucleon-

transfer channel on the shape of the potential barrier on the left.[83]

In accordance with the results of Ref. 82, the Hamiltonian of two colliding nuclei in which allowance is made for the collective quadrupole excitations in one of them is

$$\hat{H} = -\frac{\hbar^2}{2\mu}\left[\frac{\partial^2}{\partial R^2} - \frac{\hat{L}^2}{R^2}\right] + V(R) + \frac{\gamma}{R^3}\sum_{\mu}(-1)^{\mu} Y^*_{2\mu}(\Theta, \varphi)\,\alpha_{2\mu} + \hat{H}_{\text{int}}(\alpha_{2\mu}). \quad (51)$$

Here, R is the distance between the centers of mass of the colliding nuclei, $\hat{L}$ is the operator of the angular momentum of the relative motion, Θ and φ are angles which characterize the trajectory of the incident ion, and $\gamma = (3/5)Z_1Z_2e^2R_2^2$ (Z_1, Z_2 and R_1, R_2 are the charges and radii of each of the nuclei). The dynamical variables $\alpha_{2\mu}$ describe the quadrupole vibrations in the target nucleus. For the internal Hamiltonian we adopt the approximation of an effective harmonic oscillator.

The equations of motion for $\alpha_{2\mu}$ and $\partial/\partial\alpha_{2\mu}$ are

$$[\hat{H}, \alpha_{2\mu}] = -\frac{\hbar^2}{B_2}(-1)^{\mu}\frac{\partial}{\partial\alpha_{2-\mu}}; \quad (52)$$

$$\left[\hat{H}, \frac{\partial}{\partial\alpha_{2\mu}}\right] = -\frac{\gamma}{R^3}Y_{2\mu}(\Theta, \varphi) - C_2(-1)^{\mu}\alpha_{2-\mu}; \quad (53)$$

$$[\hat{H}, [\hat{H}, \alpha_{2\mu}]] = \frac{\hbar^2C_2}{B_2}\alpha_{2\mu} + \frac{\hbar^2\gamma}{B_2R^3}Y_{2\mu}(\overline{R}), \quad (54)$$

where B_2 is a mass coefficient, and C_2 is an effective rigidity.

Our aim is to obtain an effective potential in which the coupling of the relative motion to the internal vibrations of the nucleus is taken into account by a renormalization of the potential (in the general case the reduced mass μ is also renormalized[84]), i.e., we wish to obtain a Hamiltonian of the form

$$\hat{H}_{\text{eff}} = -\frac{\hbar^2}{2\mu}\left(\frac{\partial^2}{\partial R^2} - \frac{\hat{L}^2}{R^2}\right) + V_{\text{eff}}(R). \quad (55)$$

For this, we find a function $\alpha_{2\mu}(\overline{R})$ that satisfies the equation of motion (54), but with $\hat{H}$ replaced by the potential $\hat{H}_{\text{eff}}$:

$$[H_{\text{eff}}, [H_{\text{eff}}, \alpha_{2\mu}(\overline{R})]] = \frac{\hbar^2C_2}{B_2}\alpha_{2\mu}(\overline{R}) + \frac{\hbar^2\gamma}{B_2R^3}Y_{2\mu}(\overline{R}). \quad (56)$$

Then, substituting $\alpha_{2\mu}(\overline{R})$ in (51) and comparing the result of the substitution with (55), we obtain an expression for $V_{\text{eff}}(R)$. Since in this paper we do not consider corrections to the reduced mass, in the expression for the double commutator $\{\hat{H}_{\text{eff}}, [\hat{H}_{\text{eff}}, \alpha_{2\mu}(\overline{R})]\}$ we omit the terms that contain differential operators. The function can be represented in the form

$$\alpha_{2\mu}(\overline{R}) = \alpha(R)\,Y_{2\mu}(\overline{R}), \quad (57)$$

where $\alpha(R)$ is an unknown function, for which we obtain an equation by substituting (55) and (57) in (56):

$$\mu^{-1}\frac{dU_{\text{eff}}}{dR}\frac{d\alpha(R)}{dR} + \left(\frac{3\hbar}{\mu R^2}\right)^2\alpha(R) = \frac{C_2}{B_2}\alpha(R) + \frac{\gamma}{B_2R^3}. \quad (58)$$

In the interesting region of values of R greater than the sum of the half-density radii of the nuclei, and for not too light nuclei, $(3\hbar/\mu R^2)^2$ has a significantly smaller value than C_2/B_2. Therefore, in what follows we shall consider the equation

$$\mu^{-1}\frac{dU_{\text{eff}}}{dR}\frac{d\alpha(R)}{dR} = \frac{C_2}{B_2}\alpha(R) + \frac{\gamma}{B_2R^3}. \quad (59)$$

Substituting (57) in (51) and comparing the result of the substitution with (55), we obtain for U_{eff}

$$U_{\text{eff}}(R) = V(R) + \frac{5\gamma}{R^3}\alpha(R) + \frac{5}{2}C_2\alpha^2(R). \quad (60)$$

As a first approximation for $U_{\text{eff}}(R)$, we substitute the Coulomb potential in (59). Then for $\alpha_{2\mu}(R)$ we obtain the result

$$\alpha(R) = -\frac{\gamma\mu}{3B_2e^2Z_1Z_2}\exp\left(-\frac{\mu C_2R^3}{3B_2e^2Z_1Z_2}\right)\text{Ei}\left(\frac{\mu C_2R^3}{3B_2e^2Z_1Z_2}\right), \quad (61)$$

where $\text{Ei}(x)$ is the exponential integral.

It can be seen from (60) and (61) that the Coulomb turning point (for fixed collision energy E) is renormalized, leading to a more rapid decrease of the potential barrier on the right, i.e., to its narrowing and, therefore, to a growth of the below-barrier fusion cross section.

We dwell in detail on this example, since the analytic calculations are transparent and can be readily applied in calculations for specific reactions.

We consider a second question—the influence of the channels of nucleon transfer during the reaction on the behavior of the potential barrier on the left, i.e., in the region in which the nuclear forces are dominant. The final expression for the renormalized potential is cumbersome, and we refer the reader to the original paper.[83] Here we simply explain the reason for the renormalization of the potential. In accordance with the folding model, the potential energy V of the nuclear system formed by the collision of the incident ion P with the target nucleus T can be represented in the form

$$V = \int d^3x \int d^3y\,\rho(x)\,F(x, y)\,\rho(y), \quad (62)$$

where $\rho(x)$ is the density of the nucleon distribution in the nuclear system that is formed, and $F(x,y)$ is the effective interaction of the nucleons in the nuclear matter. The density $\rho(x)$ can be expressed as follows in terms of the product of field operators of the nucleons:

$$\rho(x) = \langle\Psi^+(x)\,\Psi(x)\rangle, \quad (63)$$

which, in its turn, can be approximately represented as a sum of the operators corresponding to each of the nuclei that form the system:

$$\Psi^+(x) = \Psi_P^+(x) + \Psi_T^+(x). \quad (64)$$

Substituting (64) in (63), we obtain

$$\rho = \langle\rho_P\rangle + \langle\rho_T\rangle + \langle\langle\Psi_T^+\Psi_P + \Psi_P^+\Psi_T\rangle\rangle = \rho_T + \rho_P + 2\rho_{PT}. \quad (65)$$

For the potential $V(R)$, substituting (65) in (63), we obtain

$$V(R) = V_0(R) + 4\int d^3x d^3y\,(\rho_P + \rho_T)\,F(x, y)\,\rho_{PT}, \quad (66)$$

where $V_0(R)$ is the double-folding potential.

The physical nature of the renormalization of the potential is made clear by Eq. (66). As the nuclear densities overlap, nucleons appear that belong simultaneously to the single incipient nuclear system, and this ensures an additional attraction. Calculations show[83] that the second term in (66) has a negative sign and thus leads to a sharper de-

crease of the potential barrier on the left. Thus, the sum of the two effects—the allowance for the coupling of the relative motion to the collective excitations in the entrance channel of the reaction and for the nucleon-transfer channel—leads to a narrower potential barrier, i.e., to an increase of the frequency $\hbar\omega$ [see Eq. (7)], and this indicates an enhancement of the below-barrier fusion.

Other degrees of freedom

Coupling to inelastic excitation channels and few-nucleon transfer channels is not the only possible way to enhance the probability of tunneling below the Coulomb barrier. In Ref. 19 the formation of a neck when the two nuclei make contact was proposed as an enhancement mechanism. In this model, the coupling of the ground-state channel of the incident nuclei to the neck-formation channels decreases the height of the Coulomb barrier and, therefore, increases the fusion cross section. The main argument for the introduction of this additional degree of freedom was that the fusion enhancement is approximately the same in reactions with neighboring nuclei with closed and open shells, whereas the energies and transition probabilities for the low-lying collective levels vary strongly from nucleus to nucleus. The neck-formation mechanism evidently becomes important in the fusion of heavy nuclei, for which strong overlapping of the nuclear surfaces is encountered already in the region of the Coulomb barrier. For light nuclei, this is not the case (see Fig. 5).

In Ref. 85 a further possible mechanism for increasing the tunneling probability was discussed. It was assumed that in the region of overlapping of the two nuclei the pairing gap Δ (Ref. 86) becomes a dynamical parameter, and that the potential and the mass coefficient depend on this parameter, i.e., $U_0(r) \to V_0(r,\Delta)$ and $\mu \to M(r,\Delta)$. The influence of this effect on the lifetimes of heavy nuclei against spontaneous fission and on the below-barrier fusion cross sections were estimated in the framework of the WKB method, and it was shown that the coefficient of enhancement for tunneling with a "frozen" parameter Δ is comparable with the coefficient obtained by coupling to inelastic excitation and few-nucleon transfer channels.

As we have seen, the introduction of different degrees of freedom in addition to the relative distance can increase the below-barrier fusion cross sections by several orders of magnitude. To obtain information about the importance of the various mechanisms that contribute to the enhancement, it is above all necessary to take into account the degrees of freedom that are best known.

In Ref. 87 the below-barrier fusion cross sections were investigated for reactions between various nickel isotopes. It was found that the best description of the data is obtained if one includes in the inelastic channels the second order in the parameter β_α^2 of the coupling between the channels, which arises naturally when allowance is made for the anharmonicity of the collective levels and of the ground state of the nuclei.[88] The quadratic coupling introduces additional effects not present for linear coupling. First, direct excitation of two-phonon states becomes possible. Second, a diagonal term appears in the excited channels, increasing the depth of the central potential and, therefore, decreasing the height of the Coulomb barrier. Third, a coupling between different excited channels appears. Calculations showed[87] that the shift of the fusion cross-section curve to lower energies due to allowance for the anharmonicity is comparable with the shift due to allowance for only the first order in the deformation parameter β_α. The remaining discrepancy, of 2 MeV, between theory and experiment in the ^{58}Ni + ^{64}Ni reaction is due, as we have already noted, to transfer channels with positive Q_{react}. The analogous calculations for below-barrier fusion of two ^{74}Ge nuclei still underestimate the shift of the cross section by 5 MeV (Ref. 87), indicating that additional degrees of freedom must be taken into account.

The L population of the compound nucleus

The barrier penetrability determines not only the dependence of the cross section on the energy of the incident ion, but also the penetrability of the higher partial waves for given incident energy and, therefore, the spin distribution of the compound nucleus. The spin distribution plays an important practical role in the study of fission dynamics or the synthesis of new elements. The L population of the compound nucleus influences the relative yield of neutrons, protons, α particles, and heavier nuclei and the fission products, and also the angular distributions of the fission fragments.

We now consider what changes in the L population of the compound nucleus are introduced by allowance for excited states of the colliding nuclei. In Fig. 8, which is for the ^{16}O + ^{27}Al reaction with the same set of parameters as in Fig. 6 but now with allowance for Coulomb excitation, we give the partial penetrabilities

$$F_L = (2L+1)\,|A_{\alpha L_\alpha}|^2\, k_\alpha/k_0,$$

which determine the fusion cross section in the excited channel α and in the total fusion cross section at energies 13 and 19 MeV. The broken curves are the penetrability without channel coupling, which in this case determine the total reaction cross section. It can be seen that at both energies the partial cross sections in the excited channel exhaust a large proportion of the total fusion cross section. This indicates that there is a high probability for the nuclei to be in an excited state as the critical distance is approached. Attention was first drawn to this fact in Ref. 44. We note also that even at above-barrier energies, at which allowance for channel coupling reduces the fusion cross section, the probability for formation of a compound nucleus with large angular mo-

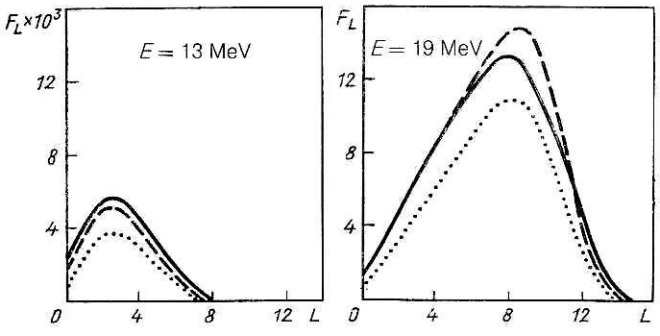

FIG. 8. Partial-wave fusion penetrabilities F_L for below-barrier and above-barrier energies for ^{16}O + ^{27}Al. The points are the penetrabilities in the excited channel; the continuous curves are the total penetrabilities in the two channels; and the broken curves are the results without channel coupling.

menta is increased. For heavier nuclei, the effect becomes still stronger. This plays an important part in the shedding of excitation by the compound nucleus, since the competition between fission and neutron evaporation for intermediate and heavy nuclei depends on the angular momentum introduced into the system.[89] For light nuclei, this leads to an increase in the probability of radiative capture, since the evaporation of neutrons with large angular momentum is difficult.

Thus, measurements of the cross sections for evaporation of neutrons, protons, α particles, light nuclei, and fission fragments (if they exist) give information about the L population of the compound nucleus. The smaller yield of neutrons from the ^{64}Ni + ^{92}Zr fusion reaction in comparison with other nuclei that lead to the same compound nucleus was explained in Ref. 90 by the high angular momenta introduced into the compound nucleus ^{156}Er.

Another way to extract the L population of the decaying nucleus is to measure the multiplicities of the photons. Usually, this information is presented in the literature[53,91] in terms of the mean angular momentum introduced into the system and is determined as follows:

$$\langle L_\gamma \rangle = \sum \sigma_{xn} \langle I_\gamma \rangle / \sum \sigma_{xn}, \tag{67}$$

where σ_{xn} is the cross section for formation of the residual nucleus after the evaporation of x neutrons, and

$$\langle I_\gamma \rangle \approx 2 (\langle M_\gamma \rangle - 4) \tag{68}$$

is expressed in terms of the mean multiplicity $\langle M_\gamma \rangle$ of the photons. The coefficients in the expression (68) reflect the fact that after evaporation of the neutrons and approximately four statistical photons the compound nucleus is de-excited by emission of quadrupole photons. In theoretical calculations, the mean angular momentum is represented in the more usual form

$$\langle L_\gamma \rangle = \sum L (2L+1) T_L / \sum (2L+1) T_L. \tag{69}$$

In Ref. 53, the photon multiplicity was measured for the previously discussed ^{16}O + ^{154}Sm reaction, and the dependence of $\langle L_\gamma \rangle$ on the energy of the incident ion was extracted. It was found that calculations using Wong's expression with $\hbar\omega = 4$ MeV and $\beta_2 = 0$ gave values which underestimated the experimental ones. Introduction of averaging over the orientations with the parameter $\beta_2 = 0.22$ reproduced not only the below-barrier fusion cross section but also the mean angular momentum $\langle L_\gamma \rangle$.

The fusion cross sections and photon multiplicities at near-barrier energies were measured in Ref. 91 for decay of the compound nucleus ^{160}Er formed in four different fusion reactions of spherical nuclei. The kinetic energy of the incident particles was chosen to give the ^{160}Er nucleus the same excitation energy in different entrance channels. Thus, the four channels differed only in the different angular momentum introduced. For asymmetric systems, the approximation (3) of a sharp cutoff with respect to the angular momentum describes the experimental data well. Allowance for the zero-point vibrations of the colliding nuclei in symmetric combinations also gives the experimental values of $\langle L_\gamma \rangle$, but the fusion cross sections were then found to be overestimated by 1.5–2 times. For the ^{80}Se + ^{80}Se reaction $\langle L_\gamma \rangle$ was measured in Ref. 92 at below-barrier energies. These results were analyzed by the method of strong channel coupling,[93] and the same result was obtained, i.e., for a correct description of $\langle L_\gamma \rangle$ the fusion cross sections were overestimated by three times.

A third way to extract the mean angular momentum is to measure the angular distributions of the fission fragments of the compound nucleus. Theoretical models[94] give for the angular distribution of the fragments the expression

$$W(\Theta) = \frac{\pi}{2k^2} \sum_L (2L+1) T_L \sum_{K=-L}^{L} (2L+1) \rho(K) \mid d^L_{0K}(\Theta) \mid^2, \tag{70}$$

where the distribution over the projection of the total spin onto the symmetry axis of the compound nucleus, $\rho(K)$, is assumed to be Gaussian,

$$\rho(K) = \exp(-K^2/2K_0^2) \left[\sum_{K=-L}^{L} \exp(-K^2/2K_0^2) \right]^{-1}, \tag{71}$$

and $K_0 = (T/\hbar^2) J_{\text{eff}}$, which is expressed in terms of the temperature T and the effective moment of inertia at the saddle point, is usually regarded as a free parameter. (There are also other parametrizations for the K distribution.[95])

In an experiment one usually measures the angular anisotropy $W(\Theta)/W(90°)$, which, as can be seen from the expression (70), depends on the L population of the compound nucleus. The investigation in Ref. 96 of the ^{160}O + ^{208}Pb reaction measured the anisotropy of the fission fragments and the fission cross section at energies at which the fission cross section is only 0.3×10^{-27} cm^2. The anisotropy was found to be much greater than expected on the basis of the one-dimensional models. The description of this experiment by the method of strong channel coupling in Ref. 97 included all levels that can be excited in this system, but a discrepancy still remained.

One further possibility for determining the L dependence of a compound nucleus of intermediate mass was proposed in Ref. 46. It was asserted that the fission cross section is more sensitive to the tails of the L distribution than is the case for the asymmetry $W(\Theta)/W(90°)$ or the γ multiplicity. In addition, the first method is suitable only for fissioning nuclei, and the second only for nuclei that are de-excited by neutron evaporation. The fission cross section was measured at below-barrier energies for the ^{58}Ni + ^{124}Sn reaction. The theoretical model of Ref. 45 [see Eq. (12)] describes the experiment well.

A new quantity characterizing fusion was measured in Ref. 98. In an experiment with aligned ^{23}Na ions on ^{48}Ti and ^{206}Pb targets the quantity T_{20}^{fus}, the tensor analyzing power for fusion, was measured in addition to the below-barrier fusion cross section. This new quantity is defined as the difference between the fusion cross sections for the different alignments of the beam of incident ions. It was found[98] that the coupling to the inelastic transfer channels makes T_{20}^{fus} smaller than in the one-dimensional models, and this permits description of the experimental data; moreover, T_{20}^{fus} was found to be more sensitive to the coupling than the fusion cross section. However, the model parameters chosen to describe T_{20}^{fus} give underestimated fusion cross sections, indicating a need to take into account few-nucleon transfer chan-

nels. However, while these last channels must contribute to the fusion enhancement, they must not change T_{20}^{fus}.

We note also that the L population of the compound nucleus also influences the variances of the fission-fragment mass distributions. It was shown in the framework of a diffusion model[99] that the variance also increases with increasing angular momentum introduced into the compound nucleus.

Thus, measurements of other characteristics, besides the fusion cross sections, of a decaying nucleus show that there are still many unresolved problems in the description of below-barrier fusion reactions.

Elastic and inelastic scattering

The multichannel models permit one to calculate not only fusion cross sections but also other processes [see Eqs. (30)–(35)], the description of which provides an independent test of the models. We shall show how coupling to the inelastic channels in the framework of the multichannel boundary-condition model changes the differential cross sections for elastic scattering at energies just above the Coulomb barrier.

Figure 9 shows the angular distributions of the elastic scattering and the partial penetrabilities T_L for the $^{16}O + {}^{27}Al$ reaction at energy 19 MeV.[21] The continuous and broken curves are the calculations with and without coupling to the 2^+ channel, respectively. The dots are the calculations made in accordance with the optical model with parameters of a real and imaginary potential of Woods–Saxon type that describe the elastic scattering at these energies.[100] We see that coupling to one low-lying level, even without the introduction of an imaginary potential, greatly improves the description of the experimental data at all angles.

We consider the possibility of simultaneous description of the fusion cross sections and total inelastic cross sections in the framework of the same model. Experiments were recently made at below-barrier energies to measure not only the fusion cross section but also the cross section for inelastic excitation of collective low-lying levels.[59,101]

The first successful attempts at a unified description of many reaction channels for the $^{16}O + {}^{208}Pb$ case were made in Ref. 97. We shall give here calculations of the cross sections of all measured reaction channels for $^{18}O + {}^{44}Ca$ collisions, made in Ref. 102.

For the $^{18}O + {}^{44}Ca$ reaction we took the nuclear part of the potential to be represented by the parametrization (14). The calculations included two excited levels of the ^{44}Ca nucleus, 2^+ and 4^+ with excitation energies 1.16 and 1.8 MeV and dynamical-deformation parameters 1.06 and 0.45 F, respectively, and the 2^+ level in the ^{18}O nucleus with energy 1.98 MeV and $\beta R = 1.01$ F. All parameters were taken from independent experiments.

In Fig. 10 the continuous curves are the fusion cross section and the cross section for excitation of the 2^+ level in the ^{44}Ca nucleus as functions of the energy of the incident ion. The experimental data are taken from Ref. 59. It can be seen that at low energies of the incident ions the excitation functions for the two nuclei differ appreciably and have different slopes, although the dynamical-deformation parameters for them are almost the same. This difference is due to the higher excitation energy for the ^{18}O nucleus and disappears at energies above the Coulomb barrier. In the same figure the dots show the fusion cross section calculated without allowance for channel coupling. In this case too the experimental data for the fusion cross section are overestimated at above-barrier energies and underestimated at below-barrier energies.

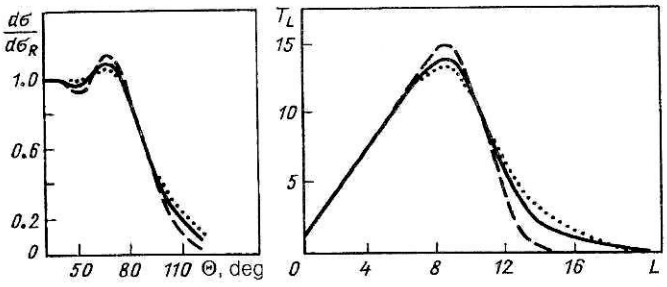

FIG. 9. Angular distributions of elastic scattering (on the left) and of the penetrability T_L (on the right) for the $^{16}O + {}^{27}Al$ reaction at energy $E = 19$ MeV. The broken curves are the calculations without channel coupling, and the dots are the calculations in accordance with the optical model.

For the $^{18}O + {}^{16}O$ reaction a good description of the experimental data of Ref. 88 for the fusion and inelastic excitation cross sections was obtained.[102]

It can be seen from the examples of this section that the boundary-condition model with coupling to the inelastic excitation channels correctly describes a wide range of experimental data for light nuclei without recourse to additional adjustable parameters. Thus, there is hope that the fusion, inelastic-scattering, and few-nucleon transfer channels for light nuclei at near-barrier energies completely exhaust all processes that in the standard optical model are described by the phenomenological imaginary potential.

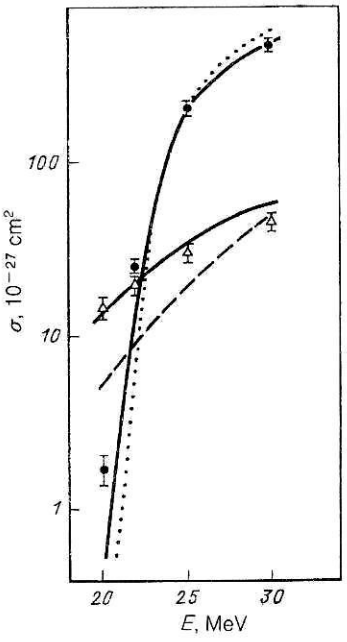

FIG. 10. Calculated cross sections for fusion and inelastic scattering with excitation of the 2^+ level in the ^{44}Ca nucleus. The experimental data are taken from Ref. 59, the broken curve gives the predictions for the excitation cross section of the 2^+ level in the ^{18}O nucleus, and the dotted curve gives the fusion cross section without channel coupling.

3. DECAY OF NUCLEI WITH EMISSION OF HEAVY CLUSTERS

We have seen that in below-barrier fusion reactions allowance for excitation of collective levels in the colliding nuclei increases the penetrability of the Coulomb barrier for heavy nuclei by an order of magnitude or more. The same effect must also be manifested in reactions with the spontaneous emission of heavy clusters, as was shown recently by perturbation-theory estimates.[103] Let us consider how tunneling in decay in the multidimensional case differs from the fusion reactions discussed earlier.

At a given energy, the penetrability of the Coulomb barrier must be different for decay and for fusion. This breaking of the penetrability symmetry when a complex particle passes through an asymmetric barrier was first pointed out in Ref. 104, in which numerical calculations were also made for potentials of the simplest shape in the one-dimensional two-channel case. In this review, we give results of calculations[105] for the physically interesting case of the decay of ^{222}Ra into ^{14}C and ^{208}Pb and the fusion of the last two nuclei.

We first formulate the boundary conditions for the system of equations (23) for decay of a heavy nucleus. At large distances, we must have outgoing waves in all channels:

$$R_\alpha(r) = S_\alpha [G_\lambda(k_\alpha r) + iF_\lambda(k_\alpha r)], \tag{72}$$

while at distance $r = R_{cr}$ we have an outgoing wave in the ground-state channel and incoming waves in all channels:

$$R_\alpha(r \simeq R_{cr}) = h_\lambda^{(1)}(k_\alpha^1 r)\,\delta_{\alpha 0} + A_\alpha h_\lambda^{(2)}(k_\alpha^1 r). \tag{73}$$

In Eqs. (72) and (73) we have eliminated the indices of the angular momentum, since the decay takes place from the ground state of the system, and the orbital angular momentum in the exit channel is determined by the multipolarity of the excited level. The part of the total flux that passes through the barrier determines the decay tunneling probability:

$$T = \sum_\alpha T_\alpha = \sum_\alpha \frac{k_\alpha}{k_\alpha^1} |S_\alpha|^2. \tag{74}$$

In numerical calculations, we took as a central potential the potential (13) with a different parametrization for γ proposed in Ref. 106: $\gamma = 1.2496[1 - (N-Z)^2/A^2]$. This potential is deeper than the standard parametrization and reproduces better the fusion barriers in the above-barrier range of energies. In the $^{14}C + {}^{208}Pb \leftrightarrow {}^{222}Ra$ reaction we take into account four excited states of the ^{208}Pb nucleus: 3^-, 5^-, 2^+, and 4^+ with excitation energies $\varepsilon_\alpha = 2.6$, 3.2, 4.1, and 4.3 MeV and dynamical-deformation parameters $\beta_\alpha R$ equal to 0.835, 0.49, 0.42, and 0.49, respectively. We have already shown the central potential and the coupling potential for this reaction, and also the configurations of the nuclei for $r = R_{cr}$ and $r = R_b$, in Fig. 5.

Figure 11 shows the energy dependences of the total penetrabilities and the various channel penetrabilities for decay, T_α, and fusion, F_α. For clarity, it is convenient to normalize them by the penetrability calculated without allowance for channel coupling. Note that the decay penetrabilities T_α shown in the figure correspond to decay from an excited ^{222}Ra nucleus, since for spontaneous decay we have $Q_{react} = 33.05$ MeV. Calculations with $E = Q_{react}$ are difficult to make with allowance for channel coupling because of the values obtained for the penetrability. Estimates

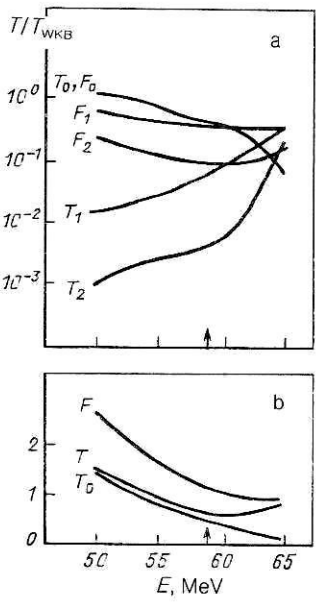

FIG. 11. a) Channel penetrabilities for decay, T_α, and fusion, F_α; b) total penetrabilities and penetrability in the ground-state channel. The arrow shows the height of the Coulomb barrier.

of it in the WKB method give $T_0(E = Q) \approx 10^{-25}$. It can be seen from Fig. 11 that at low energies the total penetrability for decay is completely determined by tunneling in the ground state, while for fusion excited channels also make an important contribution. Allowance for channel coupling enhances the penetrability for fusion already at energies $E \approx V_b$, while for decay the enhancement is slight and begins at lower energies.

The decay coefficients T_α shown in Fig. 11 give the distribution of the fluxes in the asymptotic region, while the fusion coefficients F_α give them at $r = R_{cr}$, i.e., they also take into account the redistribution of the fluxes after the Coulomb barrier has been passed.

It is interesting to establish the distances at which the redistribution of the incident flux between the various channels in the fusion and decay reactions takes place. To solve this problem, we expand the exact channel wave functions of the relative motion with respect to ingoing and outgoing waves,

$$R_\alpha(r) = f_\alpha(r)\,\Psi_\alpha^{(-)}(r) + t_\alpha(r)\,\Psi_\alpha^{(+)}(r), \tag{75}$$

for which we take their semiclassical expressions.[107] We write down functions that are normalized to unit flux and represent waves traveling to the left. In the above-barrier region they have the form

$$\Psi_\alpha^{(-)}(r) = \frac{1}{\sqrt{k_\alpha^1(r)}} \exp\left\{-i\left[\int_R^r k_\alpha^1(r')\,dr' + \pi/4\right]\right\} \tag{76}$$

and in the below-barrier region

$$\Psi_\alpha^{(-)}(r) = \frac{i}{\sqrt{|k_\alpha^1(r)|}} \exp\left\{-\left[\int_R^r |k_\alpha^1(r')|\,dr' + \pi/4\right]\right\} + \frac{1}{2\sqrt{|k_\alpha^1(r)|}} \exp\left[\int_R^r |k_\alpha^1(r')|\,dr' + \pi/4\right]. \quad (77)$$

Here, $k_\alpha^1(r)$ is the local wave number determined by the expression (28). Waves traveling to the right are obtained by complex conjugation of (76) and (77).

Assuming that in the expansion (75) the functions $\Psi_\alpha^{(-)}(r)$ and $\Psi_\alpha^{(+)}(r)$ are more rapidly varying functions of the coordinates than the coefficients $f_\alpha(r)$ and $t_\alpha(r)$, the latter can be found by matching the exact channel wave function $R_\alpha(r)$ and its derivative to the WKB functions.

Figure 12a shows, for the fusion reaction at $E = 50$ MeV, the functions $|f(r)|^2$ describing the left-moving flux in the ground-state channel and the excited channel. Figure 12b shows for the decay reaction at the same energy the functions $|t(r)|^2$ describing the right-moving flux. The arrows show the right and left turning points in the ground-state channel and excited channel for this energy. It can be seen that in the fusion reaction the system approaches the Coulomb barrier effectively unexcited, whereas for decay a large proportion of the right-moving flux is in the excited state. The reason for this is that in the fusion reaction the channel coupling before the turning point is realized by the smoothly varying Coulomb excitation potential, whereas in the decay reaction it is realized through the large and rapidly varying nuclear coupling potential (see Fig. 5).

Figure 12c shows the decay for the case when the ^{208}Pb nucleus is from the beginning in the excited 3^- state with energy 2.6 MeV and the decay occurs at energy $E = 47.4$ MeV. It can be seen that before the turning point is reached the system has a high probability of passing to the ground state, and in the asymptotic region almost all the flux is already in the ground-state channel. Thus, for calculations of the lifetime of heavy nuclei against spontaneous decay or decay from excited states, it is necessary to take into account the spectroscopic factors of configurations for which one of the decaying fragments is in the lowest excited collective states.

One may suppose that similar processes will take place in the case of single- and two-nucleon transfer reactions if the spectroscopic factors in the parent nucleus are large for certain daughter nuclei and these channels are strongly coupled to the ground-state decay channel. It is known, for example,[108] that in the ^{222}Ra nucleus the spectroscopic factor for the ^{12}C nucleus is 20 times greater than for ^{14}C, but because of the gain in Q_{react} we observe in the asymptotic region the ^{14}C nucleus, as can be seen in Fig. 12 for the analogous case of decay from the excited 3^- state.

Simple parametrizations based on microscopic calculations are given in Ref. 109 for the spectroscopic factors of heavy clusters with mass number A:

$$S(A) = S(\alpha)^{(A-1)/3},$$

where $S(\alpha)$ is the spectroscopic factor of the α particle in the parent nucleus, which is different for even and odd nuclei: $S_{\text{even}} = 6.3\times10^{-3}$ and $S_{\text{odd}} = 3.2\times10^{-3}$. Calculations of the lifetimes of heavy nuclei made in the framework of the WKB method with these spectroscopic factors[109] describe the experimental data well.

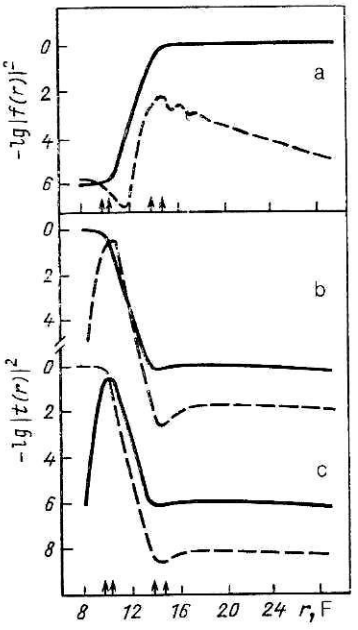

FIG. 12. Expansions of the incident flux with respect to converging and diverging waves for fusion and decay, respectively: a) fusion at energy $E = 50$ MeV; b) decay from the ground state at total energy $E = 50$ MeV; c) decay from the 3^- state at energy $E = 47.4$ MeV. The continuous curves are the fluxes in the ground-state channel, and the broken curves are in the excited channel.

Cross sections for the evaporation of heavy clusters with $Z = 3$–11 from excited nuclei were calculated in Ref. 110 in the framework of the standard evaporation model. Good agreement with the experimental data was obtained with the usual values of the parameters. The last two examples seem to support our conclusion that channel coupling does not strongly change the tunneling probability in the case of decay. However, it should be noted that the L population of the nucleus evaporating the particles is usually calculated in accordance with the optical model, for which the parameters are chosen to describe elastic scattering. Comparison of Figs. 8 and 9 shows that the mean angular momentum for T_L and F_L, which determine the partial reaction and fusion cross sections, respectively, may be different.

CONCLUSIONS

The main conclusions and results from the review are:

1. Many current models predict enhancement of the below-barrier fusion cross sections. The proposals include allowance for formation of a neck when the nuclei make contact, static deformation and zero-point vibrations for spherical nuclei, coupling to low-lying collective states and few-nucleon transfer channels, and introduction of the pairing gap as a new dynamical variable.

2. The multichannel model with strong absorption in the interior region of the nucleus is a good basis for the description of the processes that accompany the interaction of two complex nuclei at below-barrier and near-barrier energies. The parameters of the model are completely determined by the parameters of the ion–ion potentials and by the

parameters of the strength of the coupling between the various channels, which can be determined from appropriate microscopic models.

3. For light nuclei one can, without introducing additional adjustable parameters, simultaneously describe the elastic and inelastic scattering and the total fusion cross section at near-barrier and below-barrier energies. The assumptions made about the reaction mechanism are therefore sensible and enable us to confidently extrapolate the theoretical cross sections to astrophysical energies that are currently inaccessible to experimental study.

4. For intermediate nuclei the experimental data show that in the majority of cases allowance for the channels with inelastic excitation of the incident nuclei is sufficient for correct description of the below-barrier fusion cross sections.

5. Measurements of the L population of the compound nucleus give information, augmenting that from measurements of the fusion cross sections, about the reaction mechanisms at below-barrier and near-barrier energies. The impossibility of the simultaneous description of these two characteristics in some reactions when only inelastic excitation is taken into account shows that new degrees of freedom or the presence of channels with incomplete fusion of the two nuclei must be considered.

6. When many reaction channels are taken into account, the total penetrability below the Coulomb barrier is asymmetric. This can affect the description of the competition between fission and evaporation of particles as the compound nucleus sheds excitation, since the parameters of the statistical evaporation model in the exit channel are usually chosen on the basis of the inverse fusion reactions.

7. We have proposed a transparent method for separating the incident flux through the various reaction channels, and this method can also be used to analyze other processes than fusion.

It is a pleasant duty to express our gratitude to G. N. Afanas'ev, V. B. Belyaev, R. V. Jolos, F. A. Gareev, P. Medler, V. G. Solov'ev, V. D. Toneev, and R. Schmidt for helpful discussions of questions considered in the review.

[1]M. A. Kozhushner, *Tunneling Phenomena* [in Russian] (Znanie, Moscow, 1983).
[2]B. N. Zakhar'ev and A. A. Suz'ko, *Potentials and Quantum Scattering. Direct and Inverse Problems* [in Russian] (Énergoatomizdat, Moscow, 1985).
[3]I. S. Shklovskii, *Stars: Their Birth, Life, and Death* (Freeman, San Francisco, 1978) [Russ. original, Nauka, Moscow, 1984].
[4]S. G. Kadmenskiĭ and V. I. Furman, *Alpha Decay and Related Nuclear Reactions* [in Russian] (Énergoatomizdat, Moscow, 1985).
[5]A. Săndulescu, D. N. Poenaru, and W. Greiner, Fiz. Elem. Chastits At. Yadra **11**, 1334 (1980) [Sov. J. Part. Nucl. **11**, 528 (1980)].
[6]Yu. Ts. Oganessian, A. S. Iljinov, A. G. Demin, and S. P. Tretyakova, Nucl. Phys. **A239**, 353 (1975).
[7]W. Hauser and H. Feshbach, Phys. Rev. **87**, 366 (1952).
[8]J. R. Nix and A. J. Sierk, Phys. Rev. C **15**, 2072 (1977).
[9]B. N. Kalinkin and V. P. Permyakov, Preprint R4-6149 [in Russian], JINR, Dubna (1971).
[10]W. J. Swiatecki, Nucl. Phys. **A376**, 275 (1982).
[11]C. Gregorie, C. Ngo, and B. Remaud, Nucl. Phys. **A383**, 392 (1982).
[12]L. C. Vaz, J. M. Alexander, and G. R. Satchler, Phys. Rep. **69**, 373 (1981).
[13]M. Beckerman, M. Salomaa, A. Sperduto *et al.*, Phys. Rev. Lett. **45**, 1472 (1980).
[14]R. G. Stokstad, Y. Eisen, S. Kaplanis *et al.*, Phys. Rev. C **21**, 2427 (1980).
[15]C. H. Dasso, S. Landowne, and A. Winter, Nucl. Phys. **A405**, 381 (1983).
[16]P. M. Jacobs and U. Smilansky, Phys. Lett. **127B**, 313 (1983).
[17]H. Ebensen, J. Q. Wu, and G. F. Bertsch, Nucl. Phys. **A411**, 275 (1983).
[18]G. M. Berkowitz, P. Braun-Munzinger, J. S. Karp *et al.*, Phys. Rev. C **28**, 667 (1983).
[19]H. J. Krappe, K. Mohring, M. S. Nemes, and H. Rossner, Z. Phys. A **314**, 23 (1983).
[20]V. M. Shilov, in *Abstracts of Papers at the 35th Symposium on Nuclear Spectroscopy and Nuclear Structure* [in Russian] (Nauka, Leningrad, 1985), p. 446.
[21]V. M. Shilov, Communication R4-86-843 [in Russian], JINR, Dubna (1986).
[22]K. Nagatani and J. C. Peng, Phys. Rev. C **19**, 747 (1979).
[23]D. L. Hill and J. A. Wheeler, Phys. Rev. **89**, 1102 (1953).
[24]C. Y. Wong, Phys. Rev. Lett. **31**, 766 (1973).
[25]P. E. Hodgson, *The Optical Model of Elastic Scattering* (Clarendon Press, Oxford, 1963) [Russ. transl., Atomizdat, Moscow, 1966].
[26]G. R. Satchler, Nucl. Phys. **A409**, 3c (1983).
[27]R. G. Stokstad, Nukleonika **26**, 373 (1981).
[28]P. Braun-Munzinger, Nucl. Phys. **A409**, 31c (1983).
[29]J. Thomas, Y. T. Chen, S. Hinds, *et al.*, Phys. Rev. C **31**, 1980 (1985).
[30]H. A. Aljuwair, R. J. Ledoux, M. Beckerman *et al.*, Phys. Rev. C **30**, 1223 (1984).
[31]H. J. Krappe, J. R. Nix, and A. J. Sierk, Phys. Rev. C **20**, 992 (1979).
[32]M. Beckerman, Phys. Rep. **129C**, 145 (1985).
[33]A. B. Balantekin, S. E. Koonin, and L. W. Negele, Phys. Rev. C **28**, 1565 (1983).
[34]U. Jahnke, H. Rossner, D. Hilscher, and E. Holub, Phys. Rev. Lett. **48**, 17 (1982).
[35]J. Galin, M. Guerreau, M. Lefort, and X. Tarrago, Phys. Rev. C **9**, 1018 (1974).
[36]V. D. Toneev and R. Schmidt, Yad. Fiz. **27**, 1191 (1978) [Sov. J. Nucl. Phys. **27**, 631 (1978)].
[37]D. Glas and U. Mosel, Phys. Rev. C **10**, 2620 (1974).
[38]D. Glas and U. Mosel, Nucl. Phys. **A264**, 268 (1976).
[39]G. N. Afansiev, M. B. Dobromyslov, Kim Eung Poong, and V. M. Shilov, in *Proc. of the Predeal Intern. Summer School on Heavy Ion Physics* (Predeal, 1976), p. 563.
[40]G. N. Afanas'ev and V. M. Shilov, Yad. Fiz. **26**, 92 (1977) [Sov. J. Nucl. Phys. **26**, 48 (1977)].
[41]G. N. Afanas'ev, M. B. Dobromyslov, Kim Eung Poong, and V. M. Shilov, Izv. Akad. Nauk SSSR, Ser. Fiz. **41**, 1650 (1977).
[42]P. R. Christensen and Z. E. Switkowski, Nucl. Phys. **A280**, 205 (1977).
[43]T. D. Thomas, Phys. Rev. **116**, 703 (1959).
[44]G. N. Afanas'ev, V. P. Permyakov, and V. M. Shilov, *Abstracts on Papers at the 31st Symposium on Nuclear Spectroscopy and Nuclear Structure* [in Russian] (Nauka, Leningrad, 1981), p. 495.
[45]T. Udagawa and T. Tamura, Phys. Rev. C **29**, 1922 (1984).
[46]Y. Kondo, B. A. Robson, J. J. M. Bokhorst *et al.*, Phys. Rev. C **35**, 828 (1987).
[47]Y. Udagawa, B. T. Kim, and T. Tamura, Phys. Rev. C **32**, 124 (1985).
[48]G. R. Satchler and W. G. Love, Phys. Rep. **55C**, 183 (1979).
[49]J. Blocki, J. Randrup, W. J. Swiatecki, and C. F. Tsang, Ann. Phys. (N.Y.) **105**, 427 (1977).
[50]C. Ngo, B. Tamain, M. Beiner *et al.*, Nucl. Phys. **A252**, 237 (1975).
[51]V. N. Bragin and M. V. Zhukov, Fiz. Elem. Chastits At. Yadra **15**, 725 (1984) [Sov. J. Part. Nucl. **15**, 325 (1984)].
[52]R. G. Stokstad, W. Reisdorf, K. D. Hildenbrand *et al.*, Z. Phys. A **295**, 269 (1980).
[53]R. Vandenbosch, B. B. Back, S. Gil *et al.*, Phys. Rev. C **28**, 1161 (1983).
[54]M. J. Rhoades-Brown and V. E. Oberacker, Phys. Rev. Lett. **50**, 1435 (1983).
[55]H. Esbensen, Nucl. Phys. **A352**, 147 (1981).
[56]A. Bohr and B. R. Mottelson, *Nuclear Structure*, Vol. 2 (Benjamin, New York, 1975) [Russ. transl., Mir, Moscow, 1977].
[57]W. Reisdorf, F. P. Hessberger, K. D. Hildenbrand, *et al.*, Phys. Rev. Lett. **49**, 1811 (1982).
[58]R. Pengo, D. Evers, K. E. G. Lobner *et al.*, Nucl. Phys. **A411**, 255 (1983).
[59]D. M. De Castro Rizzo, E. Bozek, S. Cavallaro *et al.*, Nucl. Phys. **A427**, 151 (1984).
[60]C. H. Dasso, S. Landowne, and A. Winter, Nucl. Phys. **A407**, 221 (1983).
[61]M. J. Rhoades-Brown and P. Braun-Munzinger, Phys. Lett. **136B**, 19 (1984).
[62]G N. Afanas'ev, M. B. Dobromyslov, Kim Eung Poong, and V. M. Shilov, Izv. Akad. Nauk SSSR, Ser. Fiz. **41**, 2121 (1977).

[63]T. Tamura, Rev. Mod. Phys. **37**, 679 (1965).
[64]Yu. A. Pozdnyakov and K. O. Terenetskiĭ, Izv. Akad. Nauk SSSR, Ser. Fiz. **47**, 2187 (1983).
[65]N. F. Mott and H. S. W. Massey, *The Theory of Atomic Collisions*, 3rd ed. (Clarendon Press, Oxford, 1965) [Russ. transl., 2nd ed., IL, Moscow, 1961].
[66]R. Lindsay and N. Rowley, J. Phys. G **10**, 805 (1984).
[67]S. Landowne and S. C. Pieper, Phys. Rev. C **29**, 1352 (1984).
[68]C. H. Dasso and S. Landowne, Z. Phys. A **322**, 175 (1985).
[69]C. H. Dasso, S. Landowne, and A. Winter, Nucl. Phys. **A432**, 495 (1985).
[70]K. Alder, F. Roesel, and R. Morf, Nucl. Phys. **A284**, 145 (1977).
[71]O. Tanimura, J. Makowka, and U. Mosel, Phys. Lett. **163B**, 317 (1985).
[72]J. Q. Wu and G. F. Bertsch, Nucl. Phys. **A457**, 401 (1986).
[73]R. A. Broglia, C. H. Dasso, S. Landowne, and A. Winther, Phys. Rev. C **27**, 2433 (1983).
[74]R. A. Broglia, C. H. Dasso, and S. Landowne, Phys. Rev. C **32**, 1426 (1985).
[75]I. J. Thompson, M. A. Nagarajan, J. S. Lilley, and B. R. Fulton, Phys. Lett. **157B**, 250 (1985).
[76]W. Henning, F. L. H. Wolfs, J. P. Schiffer, and K. E. Rehm, Phys. Rev. Lett. **58**, 318 (1987).
[77]K. E. Rehm, F. L. H. Wolfs, A. M. Van den Berg, and W. Henning, Phys. Rev. Lett. **55**, 280 (1985).
[78]S. Landowne, S. C. Pieper, and F. Videbaek, Phys. Rev. C **35**, 597 (1987).
[79]W. G. Love, T. Terasawa, and G. R. Satchler, Nucl. Phys. **A291**, 183 (1977).
[80]R. V. Jolos, V. P. Permyakov, G. Repke, and G. Shul'ts, Communication E4-9670, JINR, Dubna (1976).
[81]R. V. Jolos, V. P. Permyakov, and G. Shul'ts, Preprint R4-9635 [in Russian], JINR, Dubna (1976).
[82]R. V. Jolos and V. P. Permyakov, Yad. Fiz. **47**, 58 (1988) [Sov. J. Nucl. Phys. **47**, 36 (1988)].
[83]R. V. Jolos, A. K. Nasirov, and V. P. Permyakov, Izv. Akad. Nauk SSSR, Ser. Fiz. **51**, 2041 (1987).
[84]R. V. Jolos and V. P. Permyakov, Preprint R4-6149 [in Russian], JINR, Dubna (1971).
[85]Yu. A. Lazarev, Phys. Scr. **35**, 255 (1987).
[86]V. G. Soloviev, *Theory of Complex Nuclei* (Pergamon Press, Oxford, 1976) [Russ original, Nauka, Moscow, 1971].
[87]H. Esbensen and S. Landowne, Phys. Rev. C **35**, 2090 (1987).
[88]V. V. Voronov and V. G. Solov'ev, Fiz. Elem. Chastits At. Yadra **14**, 1380 (1983) [Sov. J. Part. Nucl. **14**, 583 (1983)].
[89]S. Cohen, F. Plasil, and W. G. Swiatecki, Ann. Phys. (N.Y.) **82**, 557 (1974).
[90]D. J. G. Love, P. J. Bishop, A. Kirwan *et al.*, Phys. Rev. Lett. **57**, 551 (1986).
[91]B. Haas, G. Duchene, F. A. Beck *et al.*, Phys. Rev. Lett. **54**, 398 (1985).
[92]P. J. Nolan, D. J. G. Love, A. Kirwan *et al.*, Phys. Rev. Lett. **54**, 2211 (1985).
[93]C. H. Dasso, J. D. Garret, and S. Landowne, Phys. Lett. **161B**, 36 (1985).
[94]R. Vandenbosch and J. R. Huizenga, *Nuclear Fission* (Academic Press, New York, 1973).
[95]A. L. Barabanov and V. P. Grechukhin, Yad. Fiz. **46**, 408 (1987) [Sov. J. Nucl. Phys. **46**, 213 (1987)].
[96]T. Murakami, C. C. Sahm, R. Vandenbosch *et al.*, Phys. Rev. C **34**, 1353 (1986).
[97]S. C. Pieper, M. J. Rhoades-Brown, and S. Landowne, Phys. Lett. **162B**, 43 (1985).
[98]R. Butsch, H. Jansch, D. Kramer *et al.*, Phys. Rev. C **36**, 1351 (1987).
[99]G. D. Adeev, I. I. Gonchar, L. A. Marchenko, and N. I. Pischasov, Yad. Fiz. **43**, 1137 (1986) [Sov. J. Nucl. Phys. **43**, 727 (1986)].
[100]B. B. Back, R. R. Betts, C. Gaarde *et al.*, Nucl. Phys. **A252**, 317 (1977).
[101]J. Thomas, Y. T. Chen, S. Hinds *et al.*, Phys. Rev. C **33**, 1679 (1986).
[102]A. V. Tarakanov and V. M. Shilov, Kratk. Soobshch. OIYaI N[24]–87, 37 (1987).
[103]S. Landowne and C. H. Dasso, Phys. Rev. C **33**, 387 (1986).
[104]I. V. Amirkhanov and B. N. Zakhar'ev, Zh. Eksp. Teor. Fiz. **49**, 1097 (1965) [Sov. Phys. JETP **22**, 764 (1966)].
[105]A. V. Tarakanov and V. M. Shilov, Yad. Fiz. **48**, 109 (1988) [Sov. J. Nucl. Phys. **48**, 68 (1988)].
[106]B. B. Back, R. R. Betts, J. E. Gindler *et al.*, Phys. Rev. C **32**, 195 (1985).
[107]A. B. Migdal and V. P. Kraĭnov, *Approximation Methods in Quantum Mechanics* (Benjamin, New York, 1969) [Russ. original, Nauka, Moscow, 1966].
[108]S. G. Kadmenskiĭ, V. I. Furman, and Yu. M. Chuvil'skiĭ, in *Proc. of the School on Nuclear Structure, Alushta, 1985* [in Russian], D4-85-851, JINR, Dubna (1985), p. 385.
[109]R. Blendowske and H. Walliser, Phys. Rev. Lett. **61**, 1930 (1988).
[110]Yu. F. Muzychka and B. I. Pustyl'nik, Yad. Fiz. **45**, 90 (1987) [Sov. J. Nucl. Phys. **45**, 57 (1987)].

Translated by Julian B. Barbour